Analyses of the Stability and the Transition State of Unfolding of Hen Lysozyme using Amino Acid Mutation and X-ray Crystallography

本島, 浩之
九州大学薬学研究科医療薬学専攻

https://doi.org/10.11501/3122972

出版情報：九州大学, 1996, 博士（薬学）, 課程博士
バージョン：
権利関係：

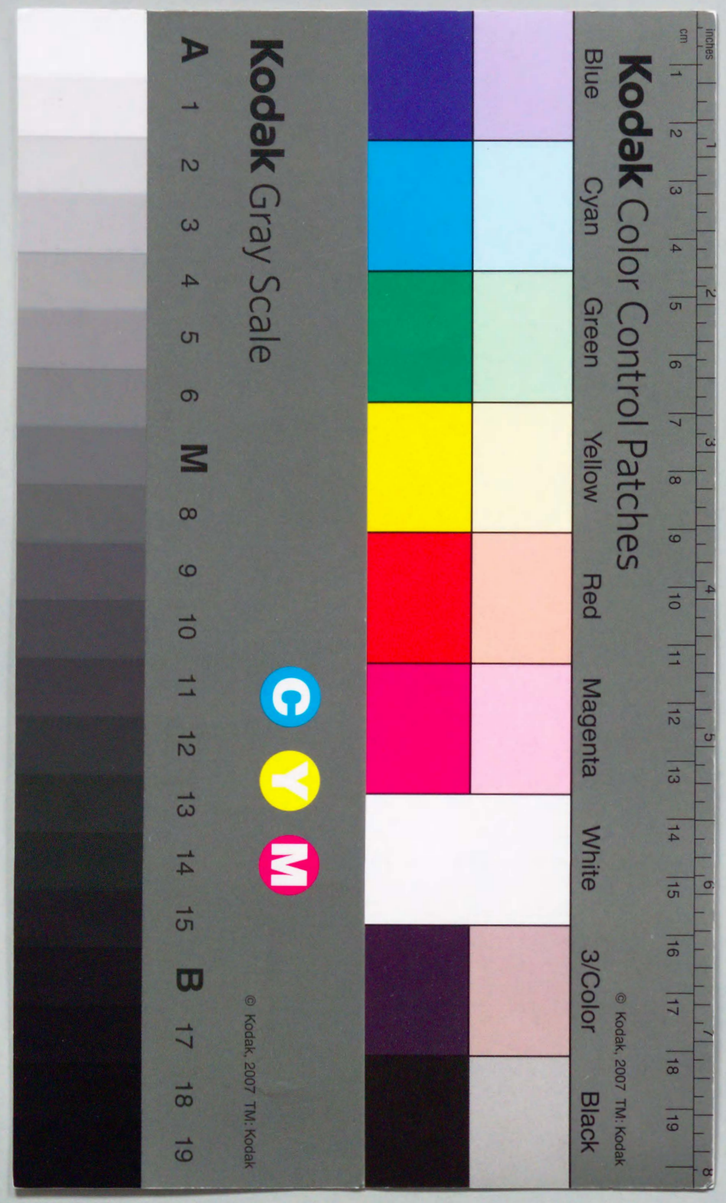

Analyses of the Stability and the Transition State of Unfolding of Hen Lysozyme using Amino Acid Mutation and X-ray Crystallography

HIROYUKI MOTOSHIMA

1997

Analyses of the Stability and the Transition State of Unfolding of Hen Lysozyme using Amino Acid Mutation and X-ray Crystallography

HIROYUKI MOTOSHIMA

1997

Abbreviations

Gdn-HCl, guanidine hydrochloride; **HPLC**, high-performance liquid chromatography; **TPCK**, L-1-(tosylamino)-2-phenylethyl chloromethyl ketone; **DSS**, 4,4-demethyl-4-silapentane-1-sulfonate; **NMR**, nuclear magnetic resonance; **DQF-COSY**, two-dimensional double-quantum-filtered J-correlated spectroscopy; **NOESY**, two-dimensional nuclear Overhauser enhancement spectroscopy.

The lysozyme Derivative

Gly47Pro47' lysozyme, a mutant lysozyme where Thr47 is mutated to a Gly-Pro sequence; **Pro47Gly47' lysozyme**, a mutant lysozyme where Thr47 is mutated to a Pro-Gly sequence; **Gly70Pro71 lysozyme**, a mutant lysozyme where Pro70Gly71 are mutated to a Gly-Pro sequence; **Gly101Pro102 lysozyme**, a mutant lysozyme where Asp101Gly102 are mutated to a Gly-Pro sequence; **Pro101Gly102 lysozyme**, a mutant lysozyme where Asp101Gly102 are mutated to a Pro-Gly sequence; **Gly117Pro118 lysozyme**, a mutant lysozyme where Gly117Thr118 are mutated to a Gly-Pro sequence; **Pro117Gly118 lysozyme**, a mutant lysozyme where Gly117Thr118 are mutated to a Pro-Gly sequence; **Gly121Pro122 lysozyme**, a mutant lysozyme where Gln121Ala122 are mutated to a Gly-Pro sequence; **Pro121Gly122 lysozyme**, a mutant lysozyme where Gln121Ala122 are mutated to a Pro-Gly sequence; **18N/27N lysozyme**, a mutant lysozyme where Asp18 is mutated to Asn; **18D/27N lysozyme**, wild-type lysozyme; **18N/27D lysozyme**, a mutant lysozyme where Asp18 and Asn27 are mutated to Asn and Asp, respectively; **18D/27D lysozyme**, a mutant lysozyme where Asn27 is mutated to Asp; **G4A lysozyme**, a mutant lysozyme where Gly4 is mutated to Ala; **G4S lysozyme**, a mutant lysozyme where Gly4 is mutated to Ser; **G4D lysozyme**, a mutant lysozyme where Gly4 is mutated to Asp; **G4E lysozyme**, a mutant lysozyme where Gly4 is mutated to Glu; **G4P lysozyme**, a mutant lysozyme where Gly4 is mutated to Pro.

CONTENTS

GENERAL INTRODUCTION

Proteins are usually in equilibrium between folded and unfolded states, and are unstable in nature and the instabilities of proteins are supposed to be involved in the physiological requirement. Thus, when we use proteins as drugs, catalysis and so on, we have better improve their stabilities. Accordingly, increasing stability of protein should be one of proposes in protein engineering. There are two methods to increase stability of a protein. In order to stabilize proteins against irreversible denaturation coupled with the unfolded state, the activation free energy for the unfolding should be increased. Under the circumstances, the information of the structure in the transition state should be collected and accumulated. However, the methods of simple analysis of protein structure in the transition state have not been established. On the other hand, the reports of protein structure in folded state have increased in recent years. This reason depends on not only the requirement of protein structures in biological science but also the advance of gene engineering and X-ray crystallography. Although the relationship between stability and structure in various proteins have been vigorously investigated, the information of this relationship is not enough yet.

Lysozyme is one of enzymes which are widely distributed in animals and plants. As three-dimensional structure of hen lysozyme was analyzed using X-ray crystallography in 1967 (*1*), the analysis of the relationship between the stability or the function and the structure in hen lysozyme have progressed. In my laboratory, the relationship have been analyzed using chemically modified lysozymed (*2-8*) or using mutation, insertion, and deletion lysozymes which are expressed from *E. Coli* (*9-10*) or *S. Cerevisiae* (*11*). In this thesis, I describe both the development of the method to analyze the structure in the transition state of hen lysozyme and the result of analysis of the stabilities of mutant lysozymes based on the structure in the folded state using X-ray crystallography.

Schimmel and Flory (*12*) have reported that prolyl residue give the conformational restriction for amino acid residue preceding the prolyl residue and the restriction for glycyl residue is smallest in all amino acid residues. Therefore, Ueda *et al.* (*13*) have reported that a Gly-Pro mutant lysozyme at 101th and 102th positions is considerably more stable than a Pro-Gly mutant lysozyme at 101th and 102th positions. In CHAPTER I, in order to determine whether or not the information obtained is applicable to other regions, I have prepared Gly-Pro and Pro-Gly mutant lysozymes at β-sheet, at loop, at β-turn, and 3_{10}-helix regions and determined those stabilities with Gdn-HCl denaturating experiment and those structures in the folded state. Since there are few report on the structure of the transition state in the unfolding of proteins , I have proposed the method to analyze the transition state in the unfolding of hen lysozyme using Gly-Pro and Pro-Gly mutant lysozymes in CHAPTER II.

On the other hand, Ishikawa *et al.* (*14*) and Watanabe *et al.* (*15*) have reported that the comparative biology is an important method to obtain the information of stability of proteins. C-type lysozyme have three α-helices (A, B, and C-helix). A surface-exposed acidic residue is located at 18th position which is spatially close to the N-terminus of B-helix. In rat, mouse-P, and mouse-M lysozymes, a buried acidic residue is present at N-cap position (residue 27) in B-helix. I have analyzed the stabilities, structures, and the pK_as of introduced Asp residues in mutant lysozymes where 18th and/or 27th positions are mutated to Asx (In CHAPTER III). Ser24 at N-cap position in B-helix and Asp88 at N-cap position in C-helix are almost conserved in the c-type lysozymes, but various amino acids exist at the N-cap position (residue 4) in A-helix. In CHAPTER IV, I have analyzed the stabilities and structures in mutant lysozymes to examine the reason why 4th position is mutated to various amino acids.

These results were published as follow:

1; Motoshima, H., Ueda, T., Hashimoto, Y., Tsutsumi, M., and Imoto, T. (1995) *J. Biochem.*, **118**, 1138-1144.

2; Motoshima, H., Ueda, T., and Imoto, T. (1996) *J. Biochem.*, **119**, 1019-1023.

3; Motoshima, H., Mine, S., Masumoto, K., Abe, Y., Iwashita, H., Hashimoto, Y., Chijiiwa, Y., Ueda, T., and Imoto, T. (1996) *J. Biochem. submitted.*

4; Motoshima, H., Masumoto, K., Hashimoto, Y., Chijiiwa, Y., Ueda, T., and Imoto. T. (1996) *J. Biochem. submitted.*

REFERENCES

1. Blake, C.C.F., Mair, G.A., North, A.C.T., Phillips, D.C. and Sarme, V.R. (1967) *Proc. Roy. Soc. London, Ser. B.*, **167**, 356-377.
2. Yamada, H., Imoto, T., and Noshita, S. (1986) *Biochemistry*, **21**, 2187-2192.
3. Kuroki, R., Yamada, H., Moriyama, T., and Imoto, T. (1986) *J. Biol. Chem.*, **261**, 13571-13574.
4. Endo, T., Ueda, T., Yamada, H., Imoto, T. (1987) *Biochemistry*, **26**, 1838-1845
5. Imoto, T., Yamada, H., Okazaki, K., Ueda, T., Kuroki, R., and Yasukouchi, T. (1987) *J. Prot. Chem.*, **6**, 95-107.
6. Ueda, T., Yamada, H., and Imoto, T., (1987) *Protein Eng.*, **1**, 189-193.
7. Yamada, H., Yamashita, T., Doumoto, H., and Imoto, T. (1990) *J. Biochem.*, **108**, 432-440.
8. Ueda, T., Yamada, H., Aoki, H., and Imoto, T. (1990) *J. Biochem.*, **108**, 886-892.
9. Miki, T., Yasukouchi, T., Nagatani, H., Furuno, M., Orita, T., Yamada, H., Imoto, T., and horiuchi, T. (1987) *Protein Eng.*, **1**, 327-332.
10. Imoto, T., Yamada, H., Yasukouchi, T., Yamada, E., Ito, Y., Ueda, T., Nagatani, H., Miki, T., and Horiuchi, T. (1987) *Protein Eng.*, **1**, 333-338.
11. Hashimoto, Y., Yamada, K., Motoshima, H., Omura, T., Yamada, H., Yasukouchi, T., Miki, T., Ueda, T., and Imoto, T (1996) *J. Biochem.*, **119**, 145-150.
12. Schimmel, P.R. and Flory, P.J. (1968) *J. Mol. Biol.*, **34**, 105-120.

13. Ueda, T., Tamura, T., Maeda, Y., Hashimoto, Y., Miki, T., Yamada, H., Imoto, T. (1993) *Protein Eng.*, **6**, 183-187.
14. Ishikawa, K., Kimura, S., Kanaya, S., Morikawa, K., and Nakamura, H. (1993) *Protein Eng.*, **6**, 85-91.
15. Wtanabe, K., Masuda, T., Ohashi, H., Mihara, H., Suzuki, Y. (1994) *Eur. J. Biochem.*, **226**, 277-283.

CHAPTER I

Correlation Between the Differences in the Free Energy Change and Conformational Energy in the Folded State of Hen Lysozymes with Gly-Pro and Pro-Gly Sequences Introduced to the Same Site

ABSTRACT

We suggested for the introduction of a prolyl residue into a protein that if the N-terminus residue is glycine, an unfavorable interaction in the folded state caused by the introduction of the prolyl residue can be substantially avoided by use of mutant lysozymes in which Gly-Pro and Pro-Gly sequences are introduced to positions 101-102 in the loop region of the lysozymes [Ueda, T., Tamura, T., Maeda, Y., Hashimoto, Y., Miki, T., Yamada, H., & Imoto, T. (1993) *Protein Engineering*, **6**, 183-187]. In order to determine whether or not the information obtained is applicable to other regions, I prepared mutant lysozymes with Gly-Pro and Pro-Gly sequences at position 47, which is located in the β-sheet, positions 70-71, which are located in the loop, positions 117-118, which are located in the β-turn, and positions 121-122, which are located in the 3_{10}-helix. The free energy changes of wild-type and mutant lysozymes for unfolding were determined at pH 5.5 and 35°C. However, a mutant lysozyme with the Gly-Pro sequence was not always more stable than that with the Pro-Gly sequence at the same site. On the other hand, in order to determine whether or not strain caused by these sequences exists in the folded or unfolded state, the structures of these mutant lysozymes were determined by use of energy minimization. On comparison of the differences in the free energy change between the mutant lysozymes with Gly-Pro and Pro-Gly sequences at the same site with those in their total local conformational energies, it was found that there is a good correlation between them. Therefore, it was suggested that the difference in total local conformational energy caused by the introduction of a Gly-Pro or Pro-Gly sequence could be estimated by use of the energy minimized structure.

Moreover, the correlation indicated that the differences in the free energy change between Gly-Pro and Pro-Gly lysozymes may be reflected by the differences in the total local conformational energies in their folded state. It was suggested that the energy levels in the unfolded states of the mutant lysozymes with Gly-Pro and Pro-Gly sequences at the same site in a Gdn-HCl solution were almost identical.

INTRODUCTION

A protein is usually in equilibrium between its folded and unfolded states. Therefore, for the stabilization of a protein against reversible denaturation, the free energy change for the unfolding should be increased by stabilizing the folded state by lowering the energy level of the folded state or by destabilizing the unfolded state by raising the energy level of the unfolded state.

Since a prolyl residue restricts the freedom of a polypeptide chain more than other amino acids, it is expected that the unfolded state of a protein should be destabilized by the introduction of a prolyl residue due to the loss of entropy. However, protein stability is not always increased on the introduction of a prolyl residue (*1*). This is mainly because the introduction of a prolyl residue often causes undesired strain in the folded state of the protein. I demonstrated that the Gly101Pro102 lysozyme, in which Asp101-Gly102 in the loop region in the lysozyme are mutated to Gly101-Pro102, became more stable than wild-type lysozyme, whereas the Asp101Pro102 lysozyme exhibited similar stability to wild-type lysozyme and the Pro101Gly102 lysozyme was markedly destabilized (2). This showed that the presence of the Gly-Pro sequence was effective for avoiding possible strain in the folded state of a protein caused by the introduction of a prolyl residue.

In this chapter, in order to determine whether or not our previous information is general, mutant lysozymes as to the β-sheet (Thr47→Gly47Pro47', Pro47Gly47'), the loop (Pro70Gly71→Gly70Pro71), the β-turn (Gly117Thr118→Gly117Pro118, Pro117Gly118), and the 3_{10}-helix (Gln121Ala122→Gly121Pro122, Pro121Gly122), were investigated (Fig. I-1).

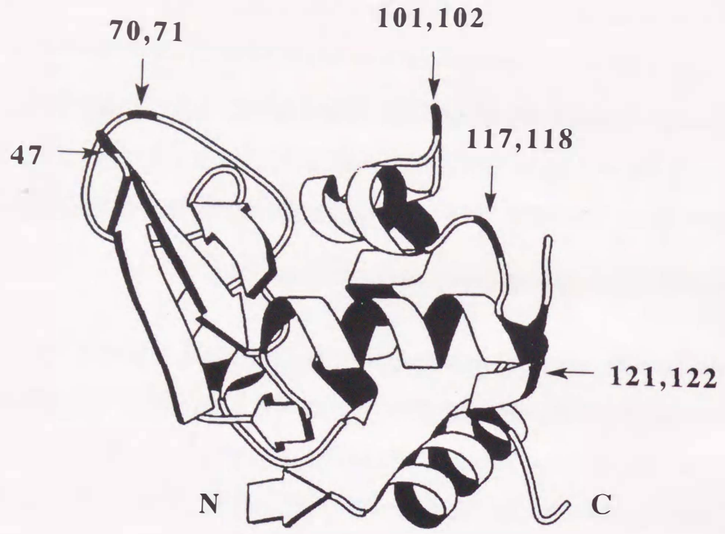

Fig. I-1. Schematic secondary and tertiary structures in hen lysozyme with the mutation sites. N and C indicate the N-terminal and C-terminal, respectively.

MATERIALS AND METHODS

Materials.

Restriction enzymes, T4 polynucleotide kinase, and DNA polymerase I (Klenow fragment) were purchased from either Takara Shuzo (Kyoto) or New England Biolabs (Beverly). *Micrococus luteus* and DNA sequencing kits (Sequenase) were purchased from Sigma and Amersham Japan (Tokyo), respectively. CM-Toyopearl 650M, a cation-exchange resin for the purification of secreted hen lysozymes, was obtained from Tosoh (Tokyo). A Wakopak $_5C_{18}$ column (mesh 200) was obtained from the Wako Pure Chemicals Institute (Osaka). The Gly101Pro102 and Pro101Gly102 lysozymes were the preparations obtained before (2). All other chemicals were of analytical grade for biochemical use.

Mutant Lysozymes.

Mutant lysozymes (Gly47Pro47', Pro47Gly47', Gly70Pro71, Gly117Pro118, Pro117Gly118, Gly121Pro122 and Pro121Gly122 lysozymes) were prepared as described before (3). The structures of the mutagenic primers used for site-

directed mutagenesis to replace Thr47 with Gly47-Pro47', Thr47 with Pro47-Gly47', Pro70-Gly71 with Gly70-Pro71, Gly117-Thr118 with Gly117-Pro118, Gly117-Thr118 with Pro117-Gly118, Gln121-Ala122 with Gly121-Pro122 and Gln121-Ala122 with Pro121-Gly122 were 5'-CAAACCGTAACGGTCCAGATGGGAGTAC-3', 5'-CAAACCGTAACCCAGGTGATGGGAGTAC-3', 5'-GGCAGGACCGGTCCATCCAGGAAC-3', 5'-CTGCAAGGGTCCAGACGTCCAG-3', 5'-CGCTGCAAGCCAGGTGACGTCCAGG-3', 5'-ACCGACGTCGGTCCATGGATCAGAG-3', and 5'-ACCGACGTCCCAGGTTGGATCAGAG-3', respectively. The mutations in the lysozyme gene were confirmed using a DNA sequence analyzer.

Purification and Identification of Lysozymes Secreted by Yeast.

Each yeast (*S. cerevisiae* AH22) transformant was cultivated at 30°C for 125 h for expression and secretion of each lysozyme by the yeast, as described before (3). Purification (ion-exchange chromatography) and identification (peptide mapping, amino acid sequencing and amino acid composition) of lysozymes secreted by the yeast were carried out as before (2).

Enzymatic Activity.

The lytic activities of lysozymes against *Micrococus luteus* were measured turbidimetrically at 450 nm, at pH 7.0 and 30°C. To a 2 ml suspension of *Micrococus luteus* in 0.05M phosphate buffer, pH 7.0, was added 50 µl of a lysozyme solution (8 - 40 µg/ml), and then the turbidity decrease was monitored at 450 nm with a Hitachi 150-20 spectrometer equipped with a thermostatically controlled cell holder. The activities of the mutant lysozyme were expressed as percentages of that of wild-type lysozyme.

Measurements of ^{1}H-NMR Spectra.

^{1}H NMR spectra were recorded at 600 MHz with a VARIAN UNITY plus spectrometer. All NMR measurements were carried out in 0.1 M CD_3COOD-NaOD at pD 5.5 with 50mM protein at 35°C. Dioxane was employed as the internal standard (3.743 ppm). The pD values were the pH meter readings without adjustment for isotope effects.

Unfolding Equilibrium.

The Unfolding equilibrium of the mutant lysozymes in Gdn-HCl was measured in 0.1 M acetate buffer at pH 5.5 and 35°C as the fluorescence at 360 nm (excitation at 280 nm). The protein concentration was 0.9 mM.

Energy Minimization.

The initial structures of these mutant lysozymes were determined by the homology modeling method starting with hen lysozyme (1HEL) from the Protein Data Bank (PDB). First, their initial structures were determined by adding the structures of the mutated region, which were constructed by use of the Homology Program developed by Biosym installed on a workstation (Indigo^2). Second, each initial structure was minimized using the Insight-Discover Program developed by Biosym installed on a workstation (Indigo^2). Energy was minimized until the norm of the gradient fell within 0.1 kcal/mol under the condition that electrostatic interaction of more than 15 Å was cut off.

Estimation of Conformational Energy.

The conformational energy was estimated for the φ angle of the introduced prolyl residue, and the ϕ and φ angles of the amino acid residue preceding the proline by use of energy contour diagrams (*4,5*) for glycyl and alanyl residues immediately succeeding the proline and prolyl residues previously reported.

RESULTS

Expression and Secretion of the Wild-type and Mutant lysozymes.

The expression and secretion of wild-type or a mutant lysozyme as a mature form by the yeast was carried out as before (*6*). The lysozymes secreted into the culture media were purified by cation-exchange chromatography. Under the conditions used, the mutant lysozymes were eluted with 0.05 M phosphate buffer containing 0.2-0.22 M NaCl, while wild-type lysozyme was eluted with 0.05 M phosphate buffer containing 0.2 M NaCl. The results indicated that each mutant lysozyme had a structure similar to that of wild-type lysozyme. The amounts of lysozyme secreted into the media were found to be 2.00, 0.03, 0.32, 1.05, 0.35, 0.48, 0.82 and 0.65 mg/l for the wild-type, Gly47Pro47', Pro47Gly47',

Gly70Pro71, Gly117Pro118, Pro117Gly118, Gly121Pro122 and Pro121Gly122 lysozymes, respectively. The amino acid compositions of these lysozymes were all consistent with those expected from the mutations introduced. In order to confirm further the mutations in the respective mutant lysozymes, they were reduced, *S*-carboxymethylated, and digested with TPCK-trypsin, and then the peptides were separated by reversed-phase HPLC. The N-terminal amino acid sequences of the peptides in question were consistent with those expected. Moreover, their amino acid compositions were also consistent with those expected. Thus, I concluded that the lysozymes secreted by the yeast here were all mature forms having the respective designed mutations.

Enzymatic activities of the mutant lysozymes.

In order to determine whether or not the tertiary structures of the mutant lysozymes were disrupted by the mutations, the enzymatic activities of the mutant lysozymes against *Micrococus luteus* were measured. Of all mutant lysozymes, the Gly47Pro47' lysozyme exhibited the lowest activity (42%), while the Pro47Gly47' lysozyme exhibited 53% activity. Since the lowest activity value was 42%, I deduced that the mutations did not cause critical structural disruptions.

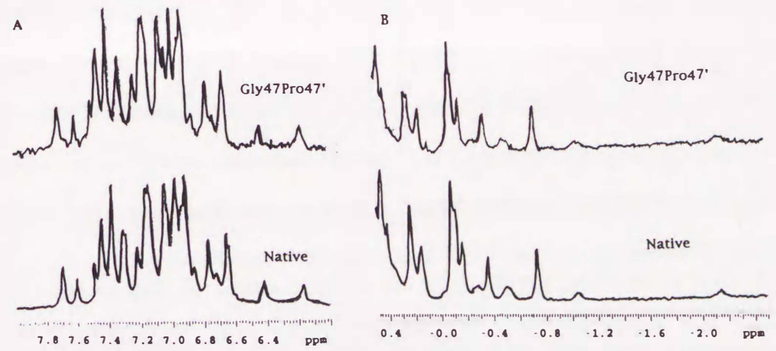

Fig. I-2. Aromatic (A) and aliphatic (B) region of ^{1}H-NMR spectra of native and the Gly47Pro47' lysozyme at pD 4.5 and 35°C.

Measurements of ^{1}H-NMR spectra of the lysozymes.

NMR is one of the means of evaluating the conformation of a protein. The ^{1}H-NMR spectra of the native and the Gly47Pro47' lysozyme with the lowest activity were measured. Since the chemical shift dispersion in the aromatic and aliphatic regions of the ^{1}H-NMR spectra of a lysozyme should be reflected in the tertiary structure, the spectra in these regions of these lysozymes are shown in Fig. I-2. Although there was a little difference in the pattern between the native and Gly47Pro47' lysozymes, the global structure of the Gly47Pro47' lysozyme with the lowest activity was suggested to be similar to that of the native lysozyme.

Stabilities of the Wild-type and the Mutant Lysozymes Determined with Gdn-HCl Denaturation.

The unfolding transitions of wild-type, Gly47Pro47', Pro47Gly47', Gly70Pro71, Gly117Pro118, Pro117Gly118, Gly121Pro122 and Pro121Gly122 lysozymes induced by Gdn-HCl were analyzed by observing changes in the tryptophyl fluorescence (emission at 360 nm, excitation at 280 nm) as a function of the denaturant concentration at pH 5.5 and 35°C (Fig. I-3). Since a lysozyme was fully unfolded in concentrated Gdn-HCl (*6*), the difference in tryptophyl fluorescence was attributed to the transition between the folded (N) and fully unfolded states (D). It was reported that the denaturation of hen lysozyme could be explained as an equilibrium between N and D on differential scanning calorimetry (*7*), and the reversibility of a protein did not change concomitant with the introduction of a prolyl residue into a protein (*8,9*). Therefore, the denaturation of these mutant lysozymes may be explained as an equilibrium between N and D. Thus, Gdn-HCl-induced denaturation curves have been analyzed by fitting the data in the equilibrated process, $N \rightleftharpoons D$ (*10*). The equilibrium constant between the folded and fully unfolded states, $K_D = D/N$, and the free energy change of unfolding, $\Delta G_D = -RT \cdot \ln K_D$, at a given concentration of Gdn-HCl were calculated from each unfolding curve. For all results reported here, ΔG_D was found to vary linearly

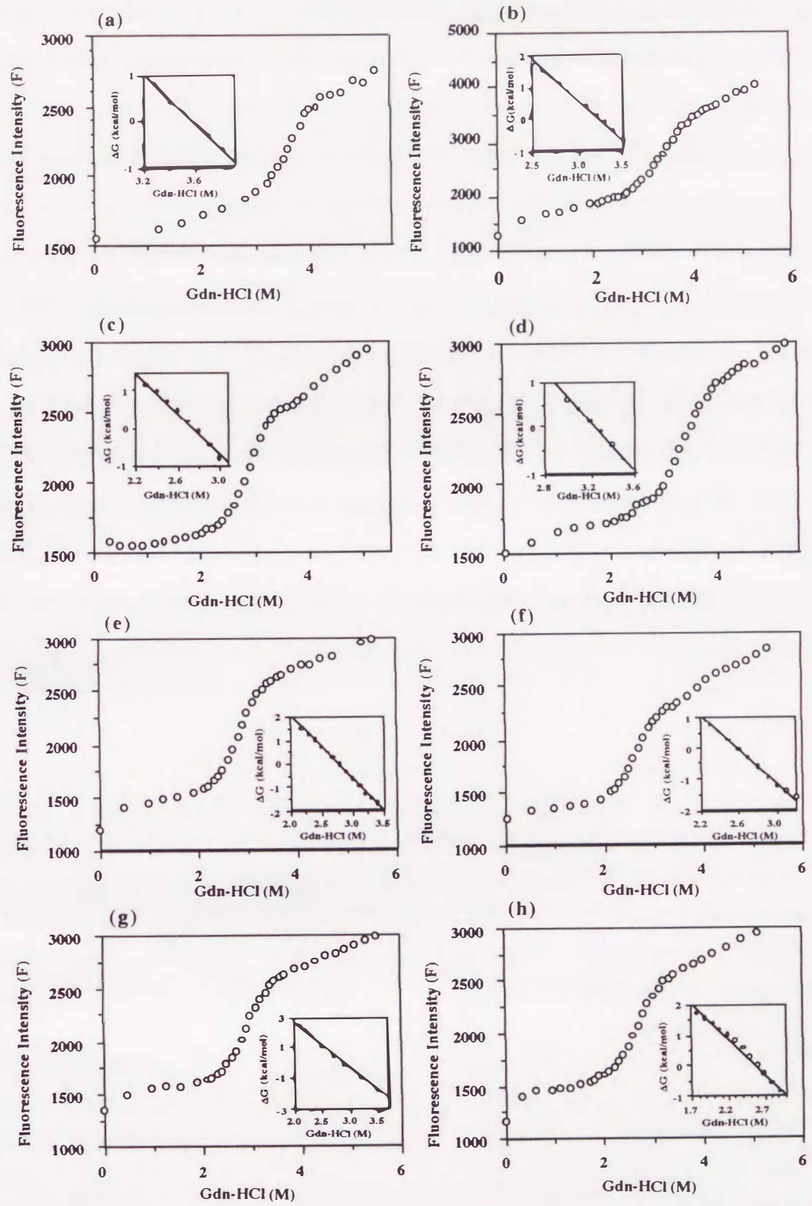

Fig. I-3. Gdn-HCl-induced denaturation curve of lysozymes measured by fluorescence at 350 nm on excitation at 280 nm in 0.1M acetate buffer at pH 5.5 and 35°C. Insets: plots of the difference between the free energies of the folded and unfolded state of lysozymes (ΔG_D) against guanidine hydrochloride concentration. (a) From wild-type lysozyme, (b) from Gly70Pro71 lysozyme, (c) from Gly47Pro47' lysozyme, (d) from Pro47Gly47' lysozyme, (e) from Gly117Pro118 lysozyme, (f) from Pro117Gly118 lysozyme, (g) from Gly121Pro122 lysozyme, (h) from Pro121Gly122 lysozyme.

with the Gdn-HCl concentration (Fig. I-3, inset), and least squares analysis was used to fit the data to the equation,

$$\Delta G_D = \Delta G_D\,(H_2O) - m\,[\text{Gdn-HCl}] \qquad (1)$$

where ΔG_D (H_2O) is the value of ΔG_D in the absence of Gdn-HCl, and m is a measure of the dependence of ΔG_D on the Gdn-HCl concentration (*10*). At the midpoint of Gdn-HCl denaturation, $C_{1/2} = \Delta G_D\,(H_2O)/m$, because $\Delta G_D = 0$ at $C_{1/2}$. The values of $C_{1/2}$ and ΔG_D (H_2O) of the respective lysozyme as well as the m values are summarized in Table I-1. The stability of a lysozyme on the introduction of the Gly-Pro sequence was higher than that on the introduction of the Pro-Gly sequence at positions 117-118 and positions 121-122, as found for positions 101-102 (*2*). However, this was not the case at positions 47-47' and positions 70-71.

Table I-1. Thermodynamic parameters characterizing the Gdn-HCl denaturation of wild-type and the mutant lysozymes at pH 5.5 and 35°C.

Lysozyme	ΔG_D (H_2O) (kcal/mol)	m (kcal/mol/M)	$C_{1/2}$ (M)
Pro47Gly47'	8.5	2.7	3.15
Gly47Pro47'	7.4	2.7	2.75
Pro70Gly71(Wild)	9.8	2.7	3.62
Gly70Pro71	8.8	2.7	3.25
Pro117Gly118	7.2	2.8	2.58
Gly117Pro118	7.8	2.8	2.77
Pro121Gly122	7.0	2.7	2.59
Gly121Pro122	8.1	2.8	2.88

Energy Minimization.

In order to compare the minimized structures of the mutant lysozymes with that of the minimized the native lysozyme, r.m.s. deviations between the mutant lysozymes and the native lysozyme were evaluated. The r.m.s. values for the total atoms and main chain atoms of the minimized structures except for the mutated residues between the mutant lysozymes and the native lysozyme were 0.56 and 0.20 for Gly47Pro47', 0.60 and 0.25 for Pro47Gly47', 0.11 and 0.10 for Gly70Pro71, 0.60 and 0.16 for Gly101Pro102, 0.58 and 0.18 for Pro101Gly102, 0.26 and 0.16 for Gly117Pro118, 0.17 and 0.13 for Pro117Gly118, 0.22 and 0.14 for Gly121Pro122 and 0.21, and 0.15 for Pro121Gly122, respectively. These results showed that the energy-minimized structures of the mutant lysozymes were similar to that of the native lysozyme. The ϕ(n) angle of the introduced prolyl residue (n), and the ϕ(n-1) and φ(n-1) angles of the amino acid residue (n-1) preceding the proline, based on their energy-minimized structures, are shown in Table I-2.

Table I-2. ϕ(n-1) and φ(n-1) angles of the amino acid residue (n-1) preceding the introducing proline and φ(n) angle of the introduced prolyl residue (n) in energy-minimized structures of the mutant lysozymes.

Lysozyme	A.A. residue (n-1)	ϕ(n-1) (degree)	φ(n-1) (degree)	φ(n) (degree)
Pro47Gly47'	Asp46	-107	153	- 70
Gly47Pro47'	Gly47	- 85	- 69	- 15
Pro70Gly71(Wild)	Thr69	- 70	120	80
70Gly71Pro	Gly70	- 64	147	55
Pro101Gly102	Ser100	- 79	- 16	17
Gly101Pro102	Gly101	- 76	-158	- 15
Pro117Gly118	Lys116	- 61	130	31
Gly117Pro118	Gly117	76	10	171
Pro121Gly122	Val120	- 61	- 18	- 33
Gly121Pro122	Gly121	- 55	- 52	- 29

Estimation of Local Conformational Energy.

In order to estimate the local conformational energies of the introduced Pro-Gly and Gly-Pro sequences, I used the φ(n) angle of the introduced prolyl residue, and the φ(n-1) and ψ(n-1) angles of the amino acid residue (n-1) preceding the proline. Namely, local conformational energies for the introduced prolyl residue [*E*(n)] and the residue preceding the proline [*E*(n-1)] were determined from ψ(n), φ(n-1) and ψ(n-1), based on the energy contour diagrams previously reported, respectively (*4,5*). The total local conformational energy (*E*) for each mutant lysozyme was represented as *E*(n)+*E*(n-1), and the differences in *E* between mutant lysozymes with the Gly-Pro and Pro-Gly sequences at the same site (Δ*E*) were represented as *E*(GP)-*E*(PG), where *E*(GP) and *E*(PG) are the total local conformational energies for mutant lysozymes with the Gly-Pro and Pro-Gly sequences, respectively. Each value is shown in Table I-3.

Table I-3. Local conformational energy and the difference in total local conformational energy in energy-minimized mutant lysozymes with Gly-Pro and Pro-Gly sequence.

Lysozyme	*E*(n-1) (kcal/mol)	*E*(n) (kcal/mol)	*E* (kcal/mol)	Δ*E* (kcal/mol)
Pro47Gly47'	1	2	3	5
Gly47Pro47'	7	1	8	
Pro70Gly71(Wild)	0	0	0	4
Gly70Pro71	0	4	4	
Pro101Gly102	7	7	14	-12
Gly101Pro102	1	1	2	
Pro117Gly118	0	4	4	-2
Gly117Pro118	1	1	2	
Pro121Gly122	7	1	8	0
Gly121Pro122	7	1	8	

It was found that the local conformation derived from the Gly-Pro sequence was more stable than that from the Pro-Gly sequence at regions 101-102 and 117-118, but not at regions 47, 70-71 and 121-122. The differences in the total local conformational energy (Δ*E*) between mutant lysozymes with Gly-Pro and Pro-Gly at the same site were plotted against those in their free energy change ($\Delta\Delta G_{obs}$) (Fig. I-4). As a result, I found a good correlation ($r^2 = 0.96$) between the differences in the free energy change ($\Delta\Delta G_{obs}$) and those in the total conformational energies (Δ*E*) in the folded states of these lysozymes.

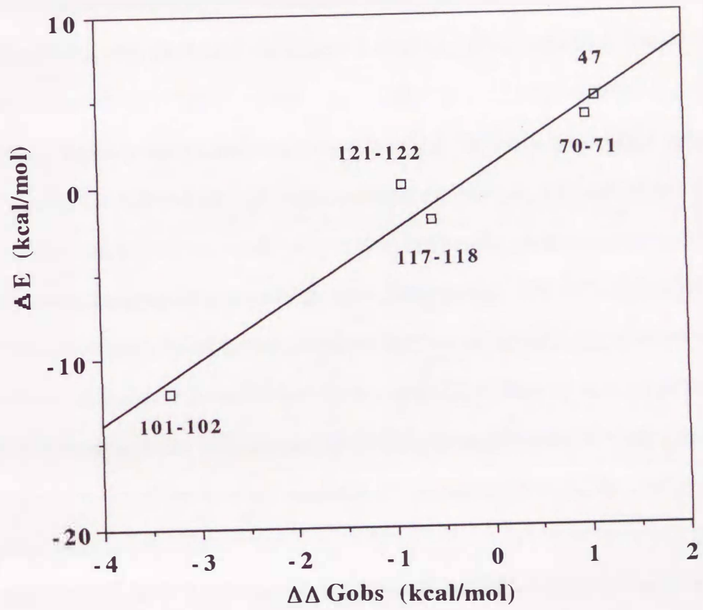

Fig. I-4. Plots of Δ*E* against $\Delta\Delta G_{obs}$ for between the mutant lysozymes with Gly-Pro and Pro-Gly sequence onto the same site.

DISCUSSION

When an amino acid replacement is made, especially in the case of amino acid insertion, it is possible that a global structural change might occur. As judged from the elution positions of the mutant lysozymes on ion-exchange

chromatography and the model structures of the mutant lysozymes, the global structures of the mutant lysozymes were similar to that of the native lysozyme. Moreover, the finding that the difference in fluorescence intensity between the folded and unfolded states of each mutant lysozyme was almost identical (Fig. I-3) confirmed that each mutation did not cause a global structural disruption. As for enzymatic activity, the Gly47Pro47' lysozyme, which has the lowest activity among mutant lysozymes examined here, exhibited 42% of the activity of the native lysozyme and the Pro47Gly47' lysozyme also exhibited lower activity (53%) than the native lysozyme. This mutation site is at the corner of the β-sheet region, where one of the active residues of lysozyme (Asp52) is located; therefore, these mutations might cause a minor local structural change leading to a decrease in the activity of the lysozyme molecule. A similar decrease in activity was observed in the mutant lysozyme in which Arg45-Asn46-Thr47-Asp48-Gly49 in the hen lysozyme mutated to Tyr45-Asn46-Ala47-Gly47'-Asp48-Arg49, which corresponds to in the case of the human lysozyme (*11*). Therefore, even in the Gly47Pro47' lysozyme, the mutation does not cause a global structural disruption. Moreover, the aromatic and aliphatic regions of the ^{1}H-NMR spectra of the Gly47Pro47' lysozyme are almost the same as those of the native lysozyme. Thus, these results supported the deduction that the global structures of the mutant lysozymes examined were similar to that of the native lysozyme.

As can be seen in Fig. I-4, there found a correlation between the differences in free energy change ($\Delta\Delta G_{obs}$) and those in the total conformational energies (ΔE) of these lysozymes in the folded state. This indicated that the differences in local conformational energy caused by the introduction of the Gly-Pro and Pro-Gly sequences could be estimated by use of the energy-minimized structures of the mutant lysozymes. As judged from the above results, even with the introduction of a glycyl residue followed by a prolyl residue, some strain in the folded state of lysozyme caused by the introduction of a prolyl residue often occurs.

In the previous paper (*2*), it was suggested that if the N-terminus residue is glycine for the introduction of a prolyl residue into a protein, an unfavorable interaction in the folded state caused by the introduction of the prolyl residue can be substantially avoided. In fact, in the mutant lysozymes in which Gly117-Thr118 and Gln121-Ala122 were converted to Gly-Pro and Pro-Gly, the mutant lysozyme with a Gly-Pro sequence at the respective site was more stable than that with a Pro-Gly sequence (Table I-2), as was found for positions 101 and 102 (*2*). Namely, the present results supported the previous finding in our laboratory that the formation of the Gly-Pro sequence is effective for avoiding the possible strain in the folded state of a protein caused by the introduction of a prolyl residue. However, in the Gly117Pro118 and Gly121Pro122 lysozymes, this stability was lower than that of wild-type lysozyme. The decrease in entropy of the main chain in a polypeptide was estimated to be 4 cal/deg/mol for the replacement of Ala with Pro (*1*). This value leads to destabilization of the unfolded state by 1.2 kcal/mol at 35°C. Therefore, in the present cases, even with the introduction of a glycyl residue followed by a prolyl residue, it was estimated that some strain in the folded state of a lysozyme caused by the introduction of glycyl and prolyl residues remained. This was supported by the finding that, in some proteins, stability as to thermal denaturation did not always increase, as had been expected, on the introduction of a prolyl residue (*1,12*).

On the other hand, the Gly47Pro47' and Gly70Pro71 lysozymes were less stable than the Pro47Gly47' and Pro70Gly71 (wild-type) ones (Table I-2). Position 47 is located in the β-turn at the corner of the β-sheet structure (*13*). In the case of a β-turn structure comprising four amino acid residues, there is a great possibility that Pro and Gly occur at the second and third positions, respectively, in the β-turn structure, and there is a small possibility that Pro occurs at the third position (*14*). Therefore, why the Gly47Pro47' lysozyme is less stable than the Pro47Gly47' one may strongly depend on the propensity to form a β-turn. In the case of the Gly117Pro118 lysozyme, in which the mutated sites are also in a local turn structure, since Gly117 and Pro118 are located at the third and fourth

positions in the turn, it is understandable from their propensities that the Gly117Pro118 lysozyme is more stable than the Pro117Gly118 one. Position 71 is located in the γ_L region (left-handed conformation) in the Pro70Gly71 (wild-type) lysozyme (*15*). Therefore, the mutation from Gly71 to Pro71(Gly→Pro) at this position might cause heavy strain due to a drastic local conformational change.

From the above results, even with the introduction of a glycyl residue followed by a prolyl residue, some strain in the folded state of a lysozyme caused by the introduction of a prolyl residue often occur. Therefore, in the case of stabilization by the introduction of a prolyl residue into a protein, it was strongly suggested that the conformations in introduced sites were serious (*1*).

Moreover, with the above good correlation I may obtain information on the unfolded state. Namely, it was suggested that the differences in the free energy change between mutant lysozymes with the Gly-Pro and Pro-Gly sequences at the same site may be caused by differences in the free energy change in their folded states. This may indicate that the energy-levels in the unfolded state of the mutant lysozymes with the Gly-Pro and Pro-Gly sequences are almost the same in a concentrated Gdn-HCl solution. This idea was supported by the finding that the polypeptide chain of a lysozyme was randomly coiled in a concentrated Gdn-HCl solution (*6*), and the restriction of movement of the main chain should greatly affect the chain entropy of the polypeptide in the unfolded state (*6*).

REFERENCES

1. Matthews, B. W., Nicholson, H., and Bechktel, W. J. (1987) *Proc. Natl. Acad. Sci. U.S.A.*, **84**, 6663-6667.
2. Ueda, T., Tamura, T., Maeda, Y., Hashimoto, Y., Miki, T., Yamada, H., and Imoto, T. (1993) *Protein Eng.*, **6**, 183-187.
3. Inoue, M., Yamada, H., Yasukochi, T., Miki, T., Horiuchi, T., and Imoto, T. (1992) *Biochemistry*, **31**, 5545-5553.
4. Schimmel, P. R. and Flory, P. J. (1968) *J. Mol. Biol.*, **34**, 105-120.

5. Vasquez, M., Nemethy, G., and Scheraga, H. A. (1983) *Macromolecules*, **16**, 1043-1049.
6. Hamaguchi, K. and Kurono, A. (1963) *J. Biochem.*, **54**, 111-122.
7. Privalov, P. L. (1979) *Adv. Protein Chem.*, **23**, 167-241.
8. Yutani, K., Ogasahara, K., Tsujita, T., and Sugino, Y. (1987) *Proc. Natl. Acad. Sci. U.S.A.*, **84**, 4441-4444.
9. Herning, T., Yutani, K., Inaka, K., Kuroki, R., Matushima, M., and Kikuchi, M. (1992) *Biochemistry*, **31**, 7077-7085.
10. Pace, C. N. (1975) *CRC Crit. Rev. Biochem.*, **3**,1-43.
11. Tomizawa, H., Yamada, H., Hashimoto, Y., and Imoto, T. (1995) *Protein Eng.*, **8**, 1023-1028.
12. Yutani, K., Hayashi, S., Sugisaki, Y., and Ogasahara, K.(1991) *Proteins*, **9**, 90-98.
13. Imoto, T., Jonson, L.N, North, A.C.T., Phillips, D.C., and Rupley, J.A. (1972) Vertebrate Lysozymes in *the Enzymes* (Boyer, P.D., ed.) Vol. 7, 3rd ed., pp. 665-868, Academic Press, New York.
14. Ishikawa, K., Kimura, S., Kanaya, S., Morikawa, K., and Nakamura, H. (1993) *Protein Eng.*, **6**, 85-91.
15. Chou, P.Y. and Fasman, G. D. (1978) *Adv. Enzymol.*, **47**, 45-147.

CHAPTER II

Analysis of the Transition State in the Unfolding of Hen Lysozyme by Introduction of Gly-Pro and Pro-Gly Sequences at the Same Site

ABSTRACT

I developed a sensitive method for analyzing the conformation of the transition state in the unfolding of hen lysozyme. The activation free energy changes of mutant lysozymes with Gly-Pro and Pro-Gly sequences at the same sites (Gly47Pro47', Pro47Gly47', Gly101Pro102, Pro101Gly102, Gly117Pro118, Pro117Gly118, Gly121Pro122 and Pro121Gly122 lysozymes) were obtained for the unfolding in aqueous solution at pH 5.5 and 35°C. Since I had shown that the difference of energies of the unfolded state in lysozymes having an introduced Gly-Pro or Pro-Gly sequence at the same site was much smaller than the difference of energies of the folded states (CHAPTER I) , the difference of energies of the folded and the transition states could be estimated unequivocally. The ϕ-value as the ratio of the difference in the free energy change in the transition state to that in the free energy change in the folded state between lysozymes with Gly-Pro and Pro-Gly sequences at the same site was defined. It gave information on how much the mutated sites retained the folded structure in the transition state. These values were 0.55 around position 47, which is located in the β-sheet structure, 0.12 at position 101-102, which is located in the loop at the upper part of the active site, 0.17 at position 117-118, which is located in the β-turn and 0.64 at position 121-122, which is located in the 3_{10}-helix. Therefore, in the transition state in the unfolding of lysozyme, it was found that a considerable portion of the structure at residues 121-122 in the 3_{10}-helix was retained in the transition state, while both the β-turn and the loop at the upper part of the active site were considerably unfolded. The β-sheet structure was also moderately disrupted in the transition state.

INTRODUCTION

To stabilize a protein against irreversible denaturation coupled with the unfolded state such as a protease digestion, kinetic stabilization is important, that is, the activation free energy for the unfolding should be increased. In our laboratory, for kinetic stabilization, it has been demonstrated to be important to stabilize a protein at a site where the local structure is largely unfolded in the transition state in the unfolding. At the same time, a method to find such sites by comparison of the thermodynamic stabilities and the unfolding rate constants for a set of modified proteins was developed (*1*). Namely, it is important to determine the structure of a protein in the transition state in the unfolding in order to stabilize the protein kinetically.

A study of the mutant lysozymes revealed that a Gly101Pro102 lysozyme was more stabilized than wild-type lysozyme, whereas a Pro101Gly102 lysozyme was markedly destabilized, though the mutations were similar (*2*). This result indicates that the formation of the Gly-Pro sequence is effective in avoiding possible strain in the folded state caused by the introduction of a proline residue, that the energy levels in the folded state of proteins might differ considerably between the mutant lysozymes with the Gly-Pro sequence and those with the Pro-Gly sequence at the same site. In CHAPTER I, I demonstrated by using activity and NMR spectra that all mutant lysozymes are folded, and suggested that the difference of energies of the unfolded state between lysozymes having an introduced Gly-Pro sequence and those with a Pro-Gly sequence at the same site was much smaller than the difference of energies of the folded states. Therefore, by comparing the ratio of the difference in the energy level in the transition state to that in the energy level in the folded state, I can estimate how much of the folded structure is retained in the transition state at a particular site.

In CHAPTER II, I analyzed the transition state in the unfolding of hen lysozyme using lysozymes with Gly-Pro and Pro-Gly sequences at the same site. The mutations are located in the β-sheet (Thr47→Gly47Pro47', Pro47Gly47'), the loop region (Asp101Gly102→Gly101Pro102, Pro101Gly102), the β-turn (Gly117Thr118→

Gly117Pro118, Pro117Gly118) and the 3_{10}-helix (Gln121Ala122→Gly121Pro122, Pro121Gly122) (Fig. II-1).

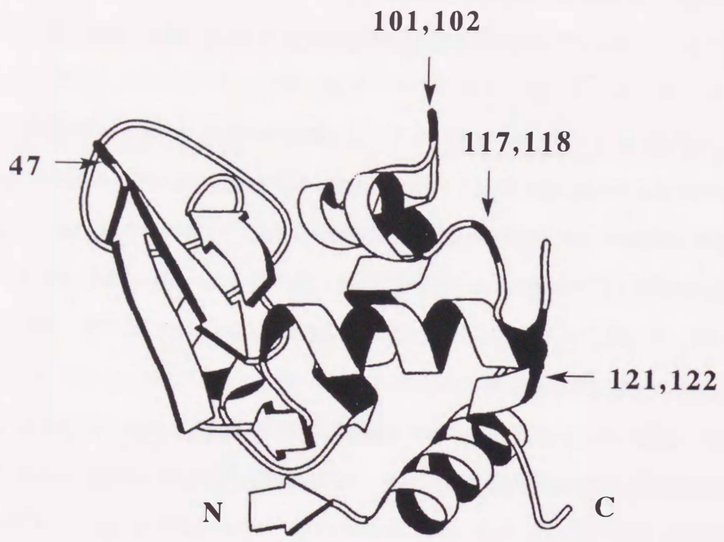

Fig. II-1. Schematic secondary and tertiary structures in lysozyme with the mutation sites. N and C indicate the N-terminal and C-terminal, respectively.

MATERIALS AND METHODS

Materials.

Gly101Pro102 lysozyme and Pro101Gly102 lysozyme were obtained as described before (2). The mutant lysozymes (Gly47Pro47' lysozyme, Pro47Gly47' lysozyme, Gly117Pro118 lysozyme, Pro117Gly118 lysozyme, Gly121Pro122 lysozyme, and Pro121Gly122 lysozyme) were obtained by the same method described in CHAPTER I. Gdn-HCl was purchased from Kanto Chemical Co. All other chemicals were of analytical grade for biochemical use.

Unfolding Kinetic Experiment.

All experiments were performed at 35°C. Unfolding was initiated by rapid dilution. Experiments were done using 1 volume of protein (9 μM) in 0.1 M acetate buffer at pH 5.5, with 10 volumes of 0.1 M acetate buffer at pH 5.5 containing concentrated Gdn-HCl. This resulted in a final Gdn-HCl

concentration between 3.5 and 6.5 M. The unfolding was followed by monitoring the intrinsic fluorescence of lysozyme using a Hitachi F-2000 fluorescence spectrophotometer (band width, 10 nm; excitation wavelength, 280 nm; emission wavelength, 350 nm). The sample solution was mixed using a mixing device fitted to the fluorescence spectrophotometer. The dead time was estimated to be 2 s.

RESULTS

Evaluation of Unfolding Rate Constants of Wild-type and Mutant Lysozymes.

The unfolding rate constant of lysozymes at pH 5.5 and 35°C was measured by Gdn-HCl jumps according to the literature (3). Even though an extra proline residue was introduced into the mutant lysozymes, their kinetic progress curves were monophasic under the conditions employed. Fig. II-2 shows plot of the logarithm of the apparent rate constants for unfolding versus the final Gdn-HCl concentration in the concentration jumps.

On the unfolded side ([Gdn-HCl] ≧3.5 - 4.5 M) in each figure, plots of log k_{app} versus [Gdn-HCl] give straight lines, indicating that k_{app} corresponds to k_u in the unfolding side (3). Thus, the unfolding rate constant in water, k_u (H_2O) was obtained, by fitting the data to the equation,

$$\log k_u = \log k_u (H_2O) - m_{ku}[\text{Gdn-HCl}] \qquad (1)$$

where m_{ku} is a measure of the dependence of $\log k_u$ on Gdn-HCl concentration (4). The values of $\log k_u$ (H_2O) for the lysozymes and the correlation factor (r) are summarized in Table II-1. Moreover, the activation free energy change ($\Delta G^{\ddagger}$) is obtained by the following equation

$$\Delta G^{\neq} = - RT \ln(h\,k)/(k_B T) \qquad (2)$$

where k_B, h, R and T are the Bolzmann constant, the Planck constant, the gas constant and temperature, respectively. The activation free energy change is also shown in Table II-1. All errors are calculated from the best fit of data.

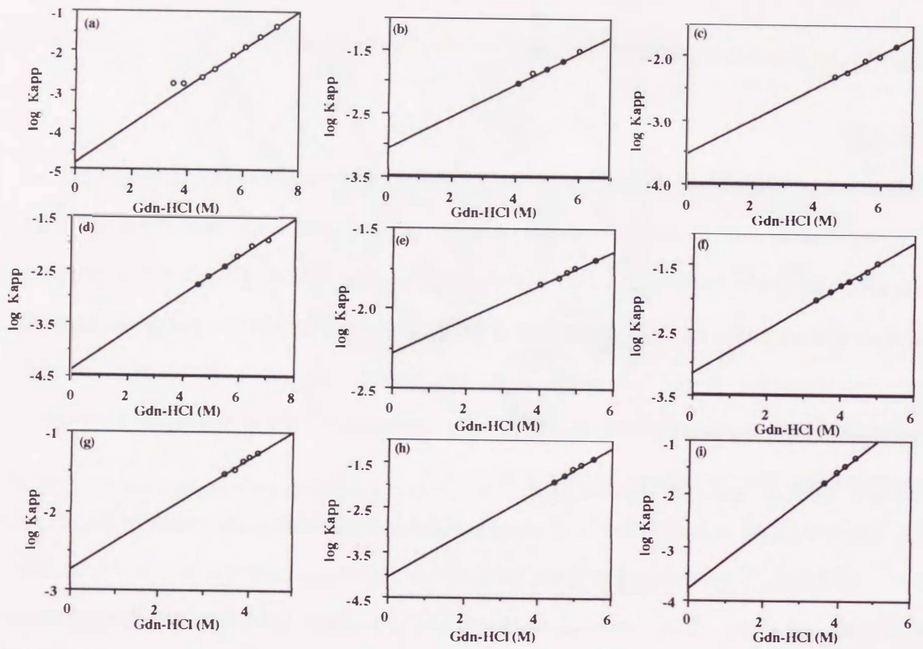

Fig. II-2. Dependence of the apparent rate constants (in s^{-1}) of unfolding on Gdn-HCl concentration in wild-type and mutant lysozymes in 0.1 M acetate buffer at pH 5.5 and 35°C. The unfolding was followed by monitoring the change in the Trp and Tyr fluorescences of lysozyme (excitation wavelength, 280 nm; emission wavelength, 350 nm). (a) Wild-type lysozyme, (b) Gly47Pro47' lysozyme, (c) Pro47Gly47' lysozyme, (d) Gly101Pro102 lysozyme, (e) Pro101Gly102 lysozyme, (f) Gly117Pro118 lysozyme, (g) Pro117Gly118 lysozyme, (h) Gly121Pro122 lysozyme, (i) Pro121Gly122 lysozyme.

Table II-1. Kinetic parameters characterizing the Gdn-HCl denaturation of wild-type and mutant lysozymes at pH 5.5 and 35°C.

Lysozyme	$\log k_u(H_2O)$ (s^{-1})	m_{ku} (M^{-1})	$\Delta G^{\neq}(H_2O)$ (kcal/mol)	r
Wild	-4.85±0.08	0.48±0.01	24.9±0.1	0.997
Gly47Pro47'	-3.06±0.06	0.25±0.01	22.4±0.1	0.993
Pro47Gly47'	-3.53±0.10	0.26±0.02	23.0±0.2	0.985
Gly101Pro102	-4.38±0.06	0.36±0.01	24.2±0.1	0.997
Pro101Gly102	-2.28±0.03	0.11±0.01	21.3±0.1	0.991
Gly117Pro118	-3.10±0.06	0.32±0.01	22.4±0.1	0.999
Pro117Gly118	-2.74±0.05	0.35±0.02	21.9±0.1	0.991
Gly121Pro122	-4.05±0.06	0.48±0.01	23.8±0.1	0.999
Pro121Gly122	-3.78±0.09	0.54±0.02	23.4±0.1	0.995

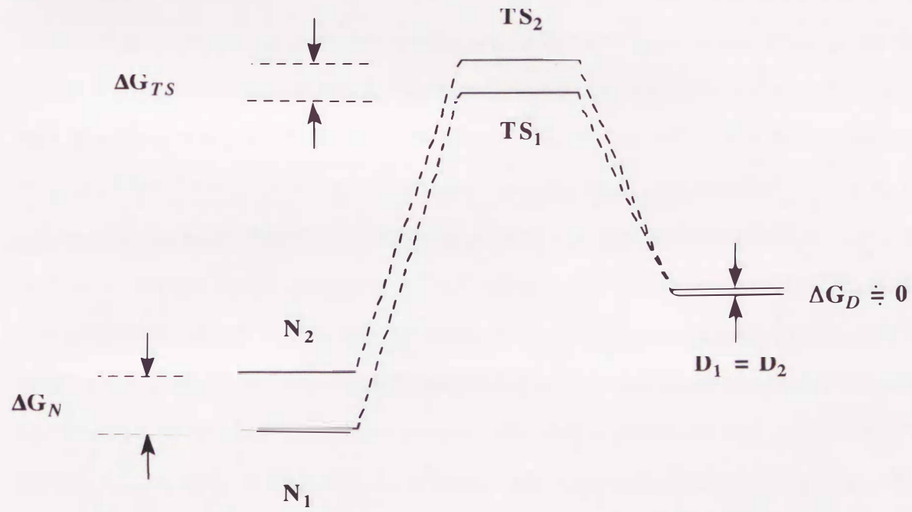

Fig. II-3. Free energy diagrams for the unfolding of mutant lysozymes at pH 5.5 and 35°C. N_1, D_1 and TS_1, and N_2, D_2 and TS_2 indicate the energy level of the folded state, the unfolded state and the transition state in mutant lysozymes in which the Gly-Pro (subscript 1) or Pro-Gly (subscript 2) sequence was introduced at the same site.

The polypeptide chain of hen lysozyme is randomly coiled in the concentrated Gdn-HCl solution (5); therefore, the restriction of the movement of the main chain should fully affect the chain entropy of the polypeptide in the unfolded state. Moreover, I had shown in CHAPTER I that the difference of energies of the unfolded state in lysozymes having an introduced Gly-Pro or Pro-Gly sequence at the same site was much smaller than the difference of energies of the folded states. WE can equate the energy level of the unfolded state of each mutant lysozyme ($D_1 \doteqdot D_2$) under the condition where $\Delta G_N >> \Delta G_D$ (Fig.II-3).

In human lysozyme, which is homologous to hen lysozyme, a stable intermediate that is thermodynamically more stable than the fully unfolded state and less stable than the folded state was observed in the unfolding coordinate between the transition state and the fully unfolded state (3). A similar stable intermediate may be also present in the unfolding of hen lysozyme. However, when I focus on the unfolding process, I can discuss the transition state in the unfolding without considering the contribution of the stable intermediate. Thus, free energy diagrams at pH 5.5 and 35°C for the unfolding of mutant lysozymes with a Gly-Pro or Pro-Gly sequence at the same site are shown in Fig. II-3 using the difference in both the free energy change in the folded state ($\Delta G_N = N_2 - N_1$) and the free energy change in the transition state ($\Delta G_{TS} = TS_2 - TS_1$) between Gly-Pro and Pro-Gly lysozymes. In the diagram, when the difference in the free energy change in the transition state between these mutants is zero, the structure at the mutated site in the transition state is similar to that in the fully unfolded state. On the other hand, when the difference in the free energy change in the transition state between these mutants is identical to that in the folded state, the structure at the mutated site in the transition state is similar to that in the folded state. Therefore, the ϕ-value that shows how close the structure at the mutated site in the transition state is to that in the folded state can be defined. It can be expressed by evaluating how much strain energy in the folded state is retained in the transition state. Namely,

$$\phi = |\Delta G_{TS}| / |\Delta G_N| \quad (3)$$

$$= |(TS_2 - TS_1)| \,/\, |(N_2 - N_1)| \quad (4)$$

$$= |[(\Delta G^{\neq}_{GP} - \Delta G^{\neq}_{PG}) - (\Delta G_{GP} - \Delta G_{PG})]| \,/\, |(\Delta G_{GP} - \Delta G_{PG})| \quad (5)$$

where ΔG_N is the difference in the free energy change for the unfolding between Gly-Pro (ΔG_{GP}) and Pro-Gly (ΔG_{PG}) mutants at each site , and ΔG_{TS} is the difference in the free energy change between ΔG_N and the difference in the activation free energy change between Gly-Pro ($\Delta G^{\neq}_{GP}$) and Pro-Gly ($\Delta G^{\neq}_{PG}$) lysozymes at each site (Table II-2). ΔG_N was evaluated in CHAPTER I. For example, in the mutant lysozyme in which Gln121-Ala122 was mutated to Gly121Pro122 and Pro121Gly122, ΔG_N and ΔG_{TS} were calculated to be 1.1 and 0.7 kcal/mol, respectively, which produced ϕ-values of 0.64. At position 121-122, 0.64 of the difference in the free energy change in the folded state between Gly121Pro122 and Pro121Gly122 lysozymes was retained in the transition state. Table II-2 shows how much of the difference in the free energy change in the folded state was retained in the transition states at each site.

Table II-2. Differences in free energy change and in activation free energy change and f-values between Gly-Pro and Pro-Gly lysozyme at pH 5.5 and 35°C.

Site	$\lvert\Delta G_N\rvert$[a] (kcal/mol)	$\lvert\Delta G_{TS}\rvert$ (kcal/mol)	ϕ-value
47	1.1	0.6	0.55
101-102	3.3	0.4	0.12
117-118	0.6	0.1	0.17
121-122	1.1	0.7	0.64

[a]The free energy changes of mutant lysozymes were obtained from CHAPTER I.

DISCUSSION

The unfolding and refolding transition of a protein is often multiphasic due to the presence of a stable intermediate (*3,4*). In human lysozyme, which is homologous to hen lysozyme, it was demonstrated that the unfolding rate constant in water, k_u (H_2O), could be evaluated from the unfolded side ([Gdn-HCl] $\geqq$3M) of the apparent rate constant even under conditions where the stable intermediate was present in the unfolding coordinate between the transition state and the fully unfolded state (*3*). Because the plots of $\log k_{app}$ versus [Gdn-HCl] above 3.5 - 4.5 M gave good straight lines for wild-type and the mutant lysozymes (Fig. II-2), I may evaluate the unfolding rate constant in water for each mutant on the basis of the dependency of $\log K_{app}$ on the unfolded side. Thus, using k_u (H_2O) for each mutant, I will discuss the kinetics of the mutant lysozymes below.

Because the polypeptide chain of hen lysozyme is randomly coiled in the concentrated Gdn-HCl solution (*5*), the restriction of movement of the main chain should fully affect the chain entropy of the polypeptide in the unfolded state. In CHAPTER I, I demonstrated by using activity and NMR spectra that all mutant lysozymes have a native-like conformation and showed that the difference of energies of the unfolded state in lysozymes having an introduced Gly-Pro or Pro-Gly sequence at the same site was much smaller than the difference of energies of the folded states. This finding made it easy to analyze energy levels of the proteins.

The gap between the energy levels of native states in the proteins having Gly-Pro and X(=not Gly)-Pro is large. The gaps (0.6 - 3.3 kcal/mol, Table II-2) may be large enough to allow calculation of the ϕ-value to analyze the transition state in the unfolding of lysozyme. Matouschek *et al.* (*4*) analyzed the transition state in the unfolding of barnase using a series of barnases mutated at the same site. In these cases, the difference in the free energy change in the folded state was derived from the difference in stability between wild-type and each mutant, and the differences in the free energy change in the folded state were not large

enough for ϕ-values to be calculated in some mutations. Therefore, the present method may have another advantage in the large difference in the free energy change in the folded state.

From the ϕ-values, it was found that the structure at residues 121-122, which is located in the 3_{10}-helix, had a similar structure to the intact one. On the other hand, the structure at residues 117-118, is located in the β-turn, and at residues 101-102, located in the loop at the upper part of the active site, are both largely unfolded in the transition state for the unfolding of lysozyme (Table II-2). Moreover, since the ϕ-value was 0.55 around residue 47, which is located in the β-sheet, the β-sheet structure was also moderately disrupted in the transition state (Table II-2). From analysis of the folding pathway of unfolded lysozyme obtained by hydrogen-exchange labeling techniques and the change in ellipticity in circular dichroism spectra, the α-helical structures have been shown to form faster than the β-sheet structure before the formation of the tertiary structure (*6*). Although I do not know whether the transition state is in the coordinate of the folding pathway, the result of Radford *et al.* (*6*) was consistent with the present result that a considerable portion of the structure at residues 121-122 in the 3_{10}-helix was retained in the transition state and the structure around residue 47 in the β-sheet was retained less. Moreover, since the formation of a considerable amount of secondary structure was estimated from the ϕ-values, the structure in the transition state was suggested to be compact, as has been reported previously (*7,8*).

From the above results, the present method was concluded to be effective for analyzing the transition state for the unfolding of lysozyme. Hereafter, using other mutant lysozymes with Gly-Pro and Pro-Gly sequences at the same site, the whole structure in the transition state of lysozyme may be able to elucidate. Moreover, the method should be applicable for analyzing the transition states of other proteins.

REFERENCES

1. Yamada, H., Ueda, T., and Imoto, T. (1993) *J. Biochem.*, **114**, 398-403.
2. Ueda, T., Tamura, T., Maeda, Y., Hashimoto, Y., Miki, T., Yamada, H., and Imoto, T. (1993) *Protein Eng.*, **6**, 183-187.
3. Herning, T., Yutani, K., Taniyama, Y. and Kikuchi, M. (1991) *Biochemistry*, **30**, 9882-9891.
4. Matouschek, A., Kellis, Jr-,J. T., Serrano, L., Bycroft, M. and Fersht, A. R. (1990) *Nature*, **346**, 440-445.
5. Hamaguchi, K. and Kurono, A. (1963) *J. Biochem.*, **54**, 111-122.
6. Radford, S. E., Dobson, C. M., and Evans, P. A. (1992) *Nature*, **358**, 302-307.
7. Segawa, S. and Sugihara, M. (1984) *Biopolymers*, **23**, 2473-2488.
8. Segawa, S. and Sugihara, M. (1984) *Biopolymers*, **23**, 2489-2498.

CHAPTER III

Analysis of the Stabilization of Hen Lysozyme with the Helix Microdipole and Charged Side Chains

ABSTRACT

In the N-terminal neighbor of the α-helix of the c-type lysozymes, two Asx residues exist at the positions of 18 and 27. Hen lysozyme has Asp18/Asn27. Therefore, I prepared three mutant lysozymes such as Asn18/Asn27, Asn18/Asp27, and Asp18/Asp27(18D/27D) lysozyme. From the comparison of the stabilities, the 18D/27D lysozyme was the most stable among the wild-type and mutant lysozymes, and the stabilization in the 18D/27D lysozyme was found to depend on the additional contribution of two dissociable residues (Asp18 and Asp27). The additivity was suggested to result from the independent contribution to the stabilization of the lysozyme such as the formation of hydrogen bonds and the charge-helix microdipole interaction from the structural analysis. Moreover, it was also suggested that the fixation of WAT1 may contribute to increased stability in the 18D/27D lysozyme. However, the extent of stabilization of the lysozyme was not quantitatively consistent with the value of pK_a of Asp18 or Asp27 in the wild-type and mutant lysozymes. Anyway, it should be the first evidence that two neighboring negative charges at the N-terminus of the helix additionally contribute to increased stability of a protein.

INTRODUCTION

The α-helix has 3.6 residues per turn and a translation per residue of 1.5Å. The α-helix can be divided into three regions; the N-terminal region, the helix center, and the C-terminal region. The main chain atoms of each amino acid unit in the helix center have two hydrogen bonds and those in the N-terminal and the C-terminal regions have one hydrogen bond.

The helix has a dipole moment with the positive pole at the N-terminus and the negative one at the C-terminus (*1*). Practically, using crystallographic data, it has been reported that Asp and Glu residue existed in the N-terminal neighborhood of the α-helix and that Lys, Arg, and His residues existed in the C-terminal neighborhood of the α-helix (*2*). Therefore, the result indicated that the electrostatic interaction between a charge and a helix dipole should take part in stabilization of a protein.

Indeed, several methods of stabilizing a protein have been submitted due to the favorable interaction at the N-terminus or the C-terminus of the helix by introducing a one-point mutation. For example, the stabilization of the α-helix in the synthetic peptide was due to the electrostatic residues at both ends (*3*). The stabilization of barnase was due to the electrostatic residue of His in the C-terminus of the α-helix (*4,5*) and the thermostabilization of T4-lysozyme was due to the electrostatic residue of Asp in the N-terminus of the α-helix (*6*). On the other hand, there was no report that double charges at the N-terminus of the helix affected the stability of a protein, although it has been demonstrated that the instability of RNase T_1 is due to the electrostatic residues of both Glu and Asp in the C-terminus of the α-helix (*7*).

In almost all of the c-type lysozymes, a surface-exposed acidic residue is located at position 18 which is near the N-terminus of the α-helix, and which extends from residues 25 to 35 (B-helix). In rat, mouse-P, or mouse-M lysozyme, a buried acidic residue is present at position 27 which is located in the N3 position of the B-helix. Two residues of 18 and 27 in hen lysozyme are Asp and Asn, respectively (Table III-1, Fig. III-1). To date, however, there have been no data on the stabilities of rat and mouse lysozymes. Therefore, in this chapter, I focus my attention on how the buried acidic residue at Asp27 contributes to the stability and how it affects the dissociable residue (Asp18) which is located near position 27, because the distance of Cγ atoms between these residues is about 10 Å based on X-ray crystallographic data. Thus, I prepared three mutant lysozymes such as Asn18/Asn27 (18N/27N), Asn18/Asp27 (18N/27D), and Asp18/Asp27 (18D/27D)

lysozyme and compared their stabilities and structures with that of the wild-type lysozyme (18D/27N) using X-ray crystallography and NMR analysis.

Table III-1. Comparison of primary structure of hen, human, mouse P, mouse M, and rat lysozyme around B-helix (25-35).

	15 * 20	* 30	40	References
HEN	HGLDNY	RGYSLGNWVC	AAKFESNFNT	20
HUMAN	L-MDG-	--I--AN-MC	LA-W--GY--	21
MOUSE P	N-MDG-	--VK-AD---	L-QH--DY--	22
MOUSE M	N-MAG-	Y-V--AD---	L-QH--DY--	23
RAT	N-MSG-	Y-V--AD---	L-QH--DY--	24
		B-helix		

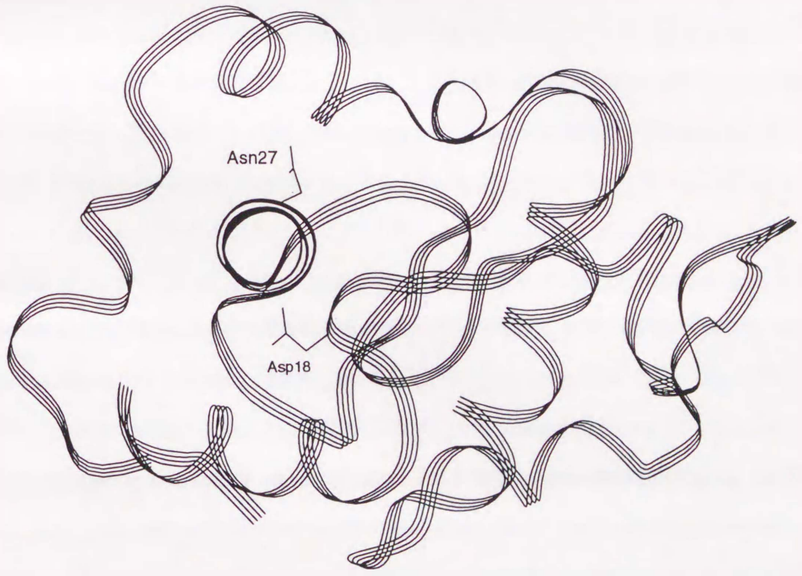

Fig. III-1. Ribbon drawing of the backbone conformation of hen lysozyme with the residues of interest. The two residues, Asp18 and Asn27, are located near the N-terminal end of the B-helix (25 - 35) in hen lysozyme.

MATERIALS AND METHODS

Materials.

Restriction enzymes, T4 polynucleotide kinase, DNA polymerase I, DNA sequencing kits, and CM-Toyopearl 650M were the same in CHAPTER I.

Purification and Identification of Lysozymes Secreted by Yeast.

Mutant lysozymes (18N/27N, 18N/27D, and 18D/27D lysozyme) were prepared and confirmed by the same procedure in CHAPTER I.

Stabilities of Mutant Lysozymes Determined with Gdn-HCl Denaturation.

Unfolding equilibria of the lysozymes by guanidine hydrochoride (Gdn-HCl) were measured according to the described procedure in CHAPTER I.

X-ray Crystallography of Mutant Lysozyme.

Mutant lysozymes were crystallized from 50 mM sodium acetate at pH 4.7 containing 0.9 -1.2 M NaCl; the conditions are same as those for crystallization of native lysozyme (*8*). The crystal was grown by vapor diffusion using the hanging-drop method. Mutant lysozymes gave isomorphous crystals with those of the wild-type lysozyme (18D/27N lysozyme). The crystals belong to the tetragonal system, space group $P4_32_12$. The intensity data out to below 2.0 Å were collected at the room temperature on a RIGAKU R-AXIS II C area detector using a RIGAKU RU-300 rotating anode source operating at 40 kV and 120 mA. The intensity data were reduced using the RIGAKU PROCESS software package. Because the mutant crystals were isomorphous to that of the wild-type crystal ($P4_32_12$, cell dimensions $a = b = 79.21$, and $c = 37.97$ Å), the coordinates of the wild-type were used as the starting model for the refinement. These structures of mutant lysozymes were refined using X-PLOR 3.1 (*9*). These structures were fitted to the Sim-weighted difference-electron density maps using the program package TURBO-FRODO 5.1 (*10*) on SGI indigo^2. The first refinements dropped the R-values of the mutant lysozymes below 23.0 %. After water molecules added to this coordinate, the next refinements were carried out. The final refinements of these structures including the water molecules gave structures of mutant lysozymes with R-values below 18.0 %. Coordinates have been assigned ID codes

in the Protein Data Bank as follows : wild-type, 1RFP; 18N/27N, 1KXW; 18N/27D, 1KXX; 18D/27D, 1KXY.

Measurement of ^{1}H-NMR.

The lysozymes were dialyzed against the solution at the measuring pH; then D_2O and NaCl were added so that the protein was in solution in 90 % H_2O : 10 % D_2O containing 5 mM NaCl. The pH values of the solution containing about 2 mM lysozyme were readjusted by adding dilute DCl or NaOD, and the pH meter readings were without correction for isotope effects (*11*). The probe temperature was calibrated with an accuracy of $\pm$ 0.2 °C using ethylene glycol. From the uncertainly in the reported pH values arising from the temperature dependence, the pH meter deviated within $\pm$ 0.1 pH unit. All chemical shifts are obtained by reference to DSS. The deviation in the measured chemical shifts is $\pm$ 0.02 ppm.

^{1}H-NMR experiments were performed on a Varain Unity 600 plus NMR spectrometer. Phase-sensitive DQF- COSY (*12*) and NOESY (*13*) experiments at pH 3.8, 35°C, were carried out at 600 MHz using the standard procedure except for pH titration. Typically 96 transients were recorded for each of 512 increments. A digital resolution of the 5.8 Hz/point in both dimensions was used for both the COSY and NOESY spectra. The assignments of the signals were carried out by reference to the literature (*14*).

RESULTS

The Stabilities of Lysozymes Determined with Gdn-HCl Denaturation.

The unfolding transitions of the wild-type lysozyme, 18N/27N, 18N/27D, and 18D/27D lysozymes induced by Gdn-HCl were analyzed by observing changes in the tryptophyl fluorescence as a function of denaturant concentration at pH 5.5 and 35°C. The denaturation of these lysozymes may be explained as an equilibrium between N and D because each lysozyme is estimated to be a one- or two-point mutant. Thus, Gdn-HCl-induced denaturation curves were analyzed by fitting the data in the equilibrated process (*15*). $\Delta G_D(H_2O)$ is the value of ΔG_D in the absence of Gdn-HCl, and m is a measure of the dependence of ΔG_D on

Gdn-HCl concentration. The midpoint of Gdn-HCl denaturation is $C_{1/2} = \Delta G_D(H_2O)/m$, because $\Delta G_D = 0$ at $C_{1/2}$. The values of $\Delta\Delta G_D(H_2O)$ are calculated using equation (1), and the average m value of the wild-type and mutant lysozymes.

$$\Delta\Delta G_D(H_2O) = \Delta G_D(H_2O)_{LYSOZYME} - \Delta G_D(H_2O)_{18N/27N} \quad (1)$$

In Table III-2, the values of $C_{1/2}$, $\Delta G_D(H_2O)$, and $\Delta\Delta G_D(H_2O)$ of the respective lysozymes as well as the m values are summarized. When the stabilities of the mutant lysozymes at pH 5.5 were compared with that of 18N/27N lysozyme, 18N/27D lysozyme was stabilized by 0.4 kcal/mol, 18D/27N lysozyme was stabilized by 0.6 kcal/mol, and 18D/27D lysozyme was stabilized by 0.9 kcal/mol. The effects of two negative charges in the 18D/27D lysozyme were found to be additive.

Table III-2. Thermodynamic parameters characterizing the Gdn-HCl denaturation of mutant lysozymes at pH 5.5 and 35°C.

Lysozyme	$C_{1/2}$ (M)	m (kcal/mol/M)	$\Delta G_D(H_2O)^a$ (kcal/mol)	$\Delta\Delta G_D(H_2O)^b$ (kcal/mol)
18N/27N	3.43±0.01	2.9	9.9	0
18D/27N (Wild)	3.62±0.01	2.7	10.5	0.6
18N/27D	3.55±0.01	3.0	10.3	0.4
18D/27D	3.74±0.01	2.9	10.8	0.9

[a]The value is determined by using the mean value of m (2.9). [b]$\Delta\Delta G_D(H_2O)$ based on the 18N/27N lysozyme.

Crystal Structures of Lysozymes.

The crystallographic data collection and refinement statistics for crystal structures of the wild-type and mutant lysozymes are summarized in Table III-3. The refined structures of the mutant lysozymes were in good agreement with that of the wild-type lysozyme. Superimposing each mutant lysozyme on the wild-type lysozyme, the root mean square (r.m.s.) deviation in the coordinates of the main chain atoms was calculated to be 0.09Å for the 18N/27N lysozyme, 0.13Å for the 18N/27D lysozyme, and 0.13Å for the 18D/27D lysozyme.

Table III-3. Crystallographic data collection and refinement statistics of lysozymes.

	18N/27N (Wild)	18D/27N	18N/27D	18D/27D
Data collections				
Cell dimensions				
a,b (Å)	79.10	79.21	79.19	79.16
c (Å)	38.16	37.97	38.00	37.88
Resolution (Å)	1.79	1.75	1.71	1.95
Unique reflections [F>1σ(F)]	10402	11948	11446	8613
Completeness (%)	86.4	93.2	83.3	93.8
R-merge (%)[a]	7.74	3.69	6.82	4.70
Refinement				
R-factor (%)[b]	17.6	16.8	17.7	16.8
Δ bond length (Å)	0.010	0.009	0.010	0.009
Δ bond angle (°)	1.509	1.448	1.493	1.472
Number of water	82 molecules	98	60	59

[a]R-merge=$\Sigma|Fi-F|/\Sigma Fi$, where Fi are repeated measurements of equivalent structure amplitudes and F is the average value of Fi. [b]R-factor=$\Sigma|Fobs-Fcalc|/\Sigma Fobs$.

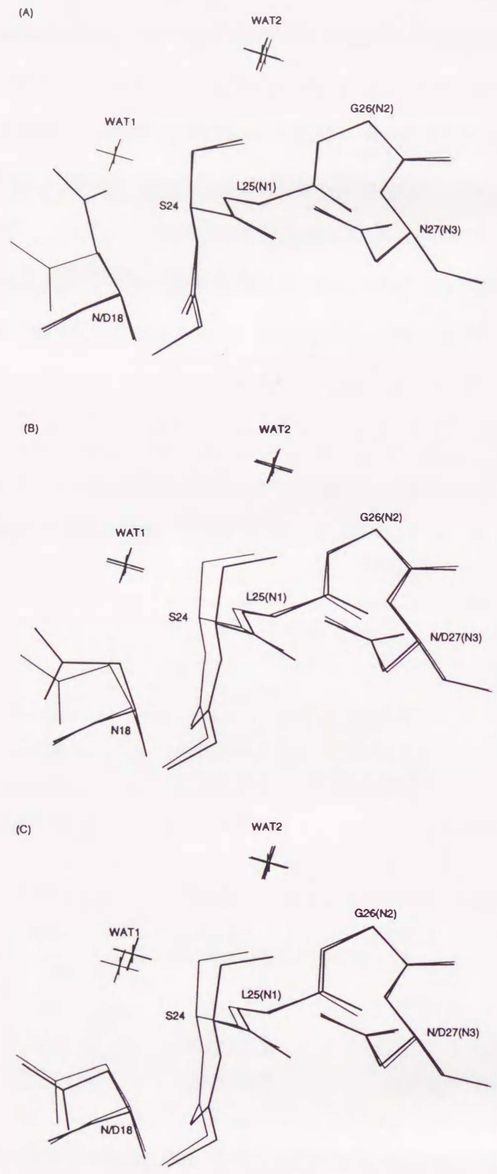

Fig. III-2. Superposition of the structure of each lysozyme (thick line) on that of 18N/27N lysozyme (thin line). (A) is 18D/27N lysozyme (wild-type), (B) is 18N/27D lysozyme, (C) is 18D/27D lysozyme. The amide groups at the position of Leu25 (N1) and Gly26 (N2) form a hydrogen bond with WAT1 and WAT2, respectively.

(1) 18D/27N Lysozyme (Wild-type): The N-terminal neighbor of the B-helix in the 18D/27N lysozyme (wild-type, thick line) is shown in Fig. III-2 (A). The amide groups at N1 and N2 positions in the B-helix in the 18D/27N lysozyme formed hydrogen bonds with the side chain of Asp18 and a water molecule (WAT2), respectively. Moreover, the negative charge at Asp18 was located at the position where the electrostatic interaction between the charge and the helix dipole in the B-helix could occur. The amide groups at N3 and N4 positions did not form hydrogen bonds.

(2) 18N/27N Lysozyme: The N-terminal neighbor of the B-helix in the 18N/27N lysozyme (thin line) is shown in Fig. III-2 (A). The amide groups at N1 and N2 positions in the B-helix in the 18N/27N lysozyme formed hydrogen bonds with two water molecules (WAT1 and WAT2). The amide groups of Leu25 (N1) in the 18N/27N lysozyme could not form a hydrogen bond with the side chain of Asp18 because the partial electron of the water's oxygen atom would be larger than that of the Oγ1 atom in the Asn residue. The amide groups at N3 and N4 positions did not form hydrogen bonds.

(3) 18N/27D Lysozyme: The N-terminal neighbor of the B-helix in the 18N/27D lysozyme (thick line) is shown in Fig. III-2 (B). The amide groups at N1 and N2 positions in the B-helix in the 18N/27D lysozyme formed a hydrogen bond with two water molecules as well as that in the 18N/27N lysozyme. A structural change at N-cap position Ser24 in the B-helix was observed in the 18N/27D lysozyme due to the introduction of the negative charge at Asp27. Moreover, the amide groups at N3 and N4 positions formed hydrogen bonds with the hydroxyl group and the carbonyl group of Ser24, respectively. The distances between atoms involved in Ser24 in the 18N/27D lysozyme are shown in Table III-4. When the formations of a hydrogen bond in both 18N/27N and 18N/27D lysozymes were examined, an acceptor atom and a donor atom in the hydrogen bond were found to exchange. Therefore, the residue Ser24 at N-cap position in the B-helix could form an end-capping structure in the 18N/27D lysozyme.

Moreover, the amide groups at N1, N2, N3, and N4 positions were confirmed to form hydrogen bonds.

Table III-4. Distances between atoms involved in Ser24 (N-cap) in B-helix of lysozymes.

		Distance (Å)			
H - acceptor	H - donor	18N/27N (Wild)	18D/27N	18N/27D	18D/27D
Asn 27 Nδ2	Ser 24 Oγ	2.73	2.94		
Ser 24 Oγ	Asp 27 Oδ1	2.83	2.65		
Ser 24 Oγ	Asn/Asp 27 N	4.04[a]	4.08[a]	3.24	3.24
Ser 24 O	Trp 28 N	3.80[a]	3.74[a]	3.29	3.29

[a]The distance is too long to form a hydrogen bond.

(4) 18D/27D Lysozyme: The N-terminal neighbor of the B-helix in the 18D/27D lysozyme (thick line) is shown in Fig. III-2 (C). A structural change at Ser24 in the 18D/27D lysozyme similar to that in the 18N/27D lysozyme was observed. The distances between atoms involved in Ser24 in the 18D/27D lysozyme are shown in Table III-4. The formation of hydrogen bonds involved in Ser24 in the 18D/27D lysozyme were identical to that of the 18N/27D lysozyme. Therefore, the residue Ser24 could form an end-capping structure in the 18D/27D lysozyme, and the amide groups at N1, N2, N3 and N4 positions were confirmed to form hydrogen bonds. On the other hand, the conformation of Asp18 in the 18D/27D lysozyme (Fig. III-2 (C), thick line) was different from that in the 18D/27N lysozyme (Fig. III-2 (A), thick line). The side chain of Asp18 was considered to change its position allowing the amide group of Leu25 (N1) to form a hydrogen bond with WAT1 because of the electrostatic repulsion between Asp18 and Asp27 in the 18D/27D lysozyme. Fig. III-3 shows hydrogen bonds at Asp18 in the

18D/27D lysozyme. The hydrogen bonds are formed between the side chain of Asp18 and that of Arg128 in a neighboring molecule. This may be the result of the side chain at Asp18 having taken a different orientation in the 18D/27D lysozyme from that in the wild-type lysozyme.

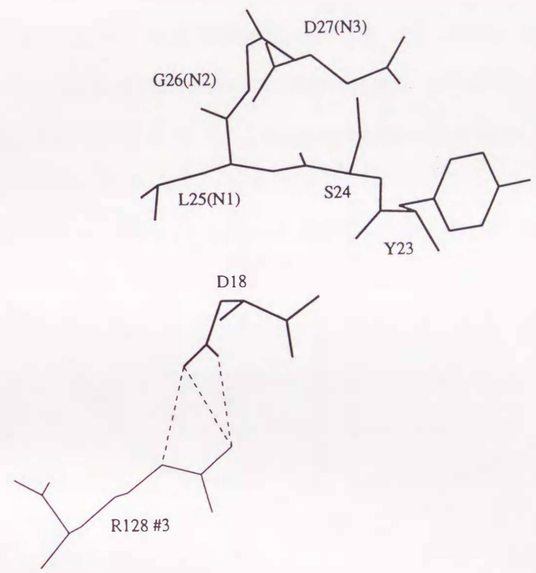

Fig. III-3. The crystal structure of the region near the N-terminus of the B-helix (25-35) in 18D/27D lysozyme (thick line). The hydrogen bonds between the Asp18 side chain and the Arg128 side chain of a neighboring molecule (thin line) were observed.

pK_a of Asp18 and Asp27 in Lysozymes.

To determine the pK_a of Asp18 and Asp27, the measurements of 600 MHz ^{1}H-NMR spectra were conducted at 35°C and various pH values (1.5 - 7.5). The resonances of Asp18 βCH and Trp111 indole protons were employed to determine the dissociation of Asp18 and Asp27 in each lysozyme because Asp27 forms a hydrogen bond with the N-1 proton of Trp111 and because they were separated from other resonances. These resonances were assigned using the respective ^{1}H-^{1}H COSY and ^{1}H-^{1}H NOSEY spectra. In Fig. III-4, the measured

chemical shifts are plotted against pH. The curve-fitting analysis for the pK_a of Asp18 or Asp27 was carried out for the pH dependence of the signal. As a result, it was found that the pK_a of Asp18 in the 18D/27N lysozyme (wild-type) was 2.3 (*16*), the pK_a of Asp27 in the 18N/27D lysozyme was below 2.2, and the pK_a of Asp18 and Asp27 in the 18D/27D lysozyme were 3.3 and 2.9, respectively (Table III-5). All pK_a values of Asp18 and Asp27 in the mutant lysozymes were lower than 4.0 which is the intrinsic value for the Asp residue. These results indicated that favorable electrostatic interactions were present at the position of Asp18 and Asp27 in the wild-type and mutant lysozymes.

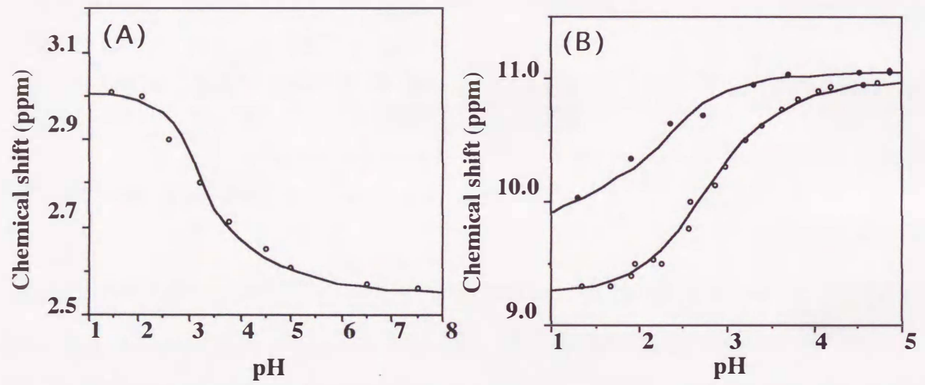

Fig. III-4. pH dependence of the chemical shifts of (A) the βCH proton of Asp18 in 18D/27D (opened circle) lysozyme, and of (B) indole proton of Trp111 in 18N/27D (closed circle) and 18D/27D (opened circle) lysozymes. Asp27 in both 18N/27D and 18D/27D lysozymes forms a hydrogen bond with the indole proton of Trp111.

Table III-5. pK_a of Asp18 and Asp27 in lysozymes.

	18N/27N	18D/27N (Wild)	18N/27D	18D/27D
Asp18	----	2.3[a]	----	3.3
Asp27	----	----	<2.2	2.9

[a]The value is referred to Abe *et al.*, 1995.

Analysis of B-helix Structure by Two-Dimensional ^{1}H-NMR in 18D/27D Lysozyme.

In order to analyze the secondary structure around the B-helix in the 18D/27D lysozyme in solution, which is the most stable lysozyme employed here, the assignments of the chemical shifts around the region in the mutant lysozyme were carried out. On the other hand, the chemical shifts of the resonances in the wild-type lysozyme were used from the previous literature (*14*). Fig. III-5 shows the chemical shift indexes of αCH in the wild-type and 18D/27D lysozymes at pH 3.8. The assignment of a secondary structure in a protein was carried out according to the literature (*17*). The results indicated that Ser24 in the 18D/27D lysozyme had a β-conformation while that in wild-type lysozyme did not. This was consistent with the results of the crystal structure. Fig. III-6 showed the NOE connectivities of 23 - 36 amino acid residues in the wild-type and 18D/27D lysozymes at pH 3.8. The NOE between αCH of Leu25 (N1) and NH of Trp28 (N4) was observed in the 18D/27D lysozyme, however, it was not observed in the wild-type lysozyme.

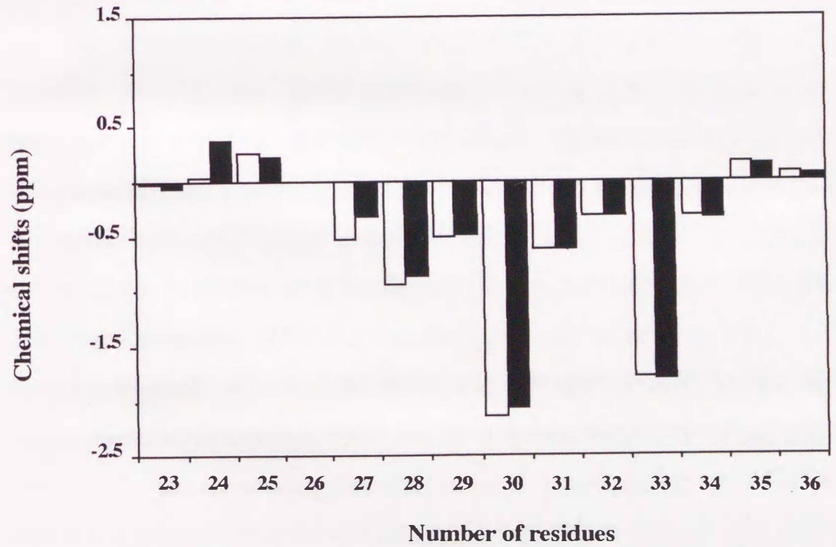

Fig. III-5. Chemical shift index of αCH in wild (opened bar) and 18D/27D (closed bar) lysozymes at pH 3.8.

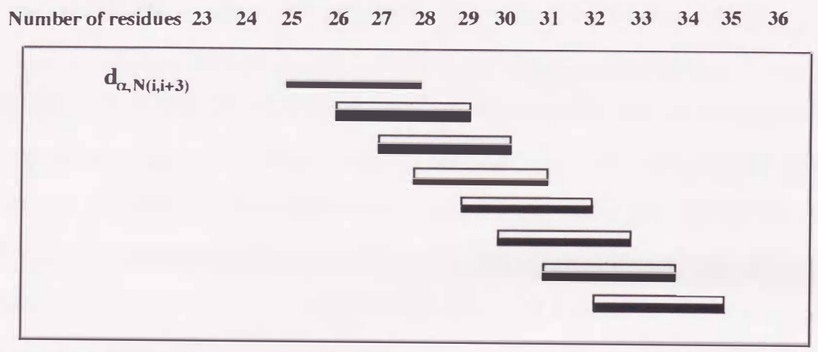

Fig. III-6. The NOE connectivities of 23 - 36 amino acid residues of wild (opened bar) and 18D/27D (closed bar) lysozymes at pH 3.8.

DISCUSSION

Because the pK_a of Asp18 was lower than the intrinsic pK_a of Asp from the titration experiment of the lysozyme using NMR (*16*), I supposed that the negative charge at Asp18 contributed to stabilizing the lysozyme. As was expected, the 18N/27N lysozyme was less stable than the wild-type (18D/27N) lysozyme. On the other hand, the 18D/27D and 18N/27D lysozymes were more stable than the 18N/27N lysozyme while the side chain at the position of 27 was less accessible to the solvent. This was confirmed by the result that the pK_as of Asp27 in these mutant lysozymes were lower than the intrinsic pK_a of Asp (4.0). The observation should be strange because the carboxyl groups on the inside of a protein molecule are hard to dissociate. For example, Glu35 in the lysozyme, which is located in the inside of lysozyme, has a higher pK_a (6.1) than the intrinsic one (*18*). From X-ray analysis, the dissociated side chain of Asp27 at N3 position in the B-helix in these mutant lysozymes formed a hydrogen bond with Ser24 at N-cap position on the B-helix. The observation from the NMR measurement of the 18D/27D lysozyme at pH 3.8 supported this X-ray result, such as the structural change around Ser24 and the appearance of a new NOE. Therefore, the side chain of Asp27 may be present in dissociated form under the

conditions of X-ray crystallographic analysis (pH 4.7) and the conditions of the stability measurement (pH 5.5).

Zhukovsky *et al.* (*19*) demonstrated that a hydrogen bond between the side chain of the residue that is located at N-cap position in the α-helix and the backbone of the residue that is located at N3 position in the α-helix contributed to stabilizing a protein. However, in the wild-type (18D/27N) lysozyme, the hydrogen bond between the side chain at the N-cap position Ser24 and the backbone at N3 position Asn27 in the B-helix would not contribute to stabilizing the lysozyme because this distance is too long to form a hydrogen bond. On the other hand, in the 18N/28D and 18D/27D lysozymes, the distances between the side chain at N-cap position Ser24 and the backbone at N3 position Asp27 in the B-helix became close enough to form hydrogen bonds due to the dissociation of aspartic acid at N3 position Asp27. From these results, I concluded that the favorable interaction in the N-terminus of the B-helix by the dissociable residue introduced contributed to increased stability of the lysozyme.

As was stated above, because the pK_a of Asp18 was lower than the intrinsic pK_a of Asp (4.0), the residue was expected to contribute to stabilizing the lysozyme. I wonder if the introduction of a new negative charge near the Asp18 may affect the dissociation of Asp18, resulting in a decrease in the stability of the lysozyme. The result obtained has indicated that these aspartic residues surely interacted with each other in solution. This interaction may induce the structural change at the side chain of Asp18 in the 18D/27D lysozyme (Fig. III-2 (C)), and the side chain formed hydrogen bonds with Arg128 of the neighboring molecule (Fig. III-3). However, the 18D/27D lysozyme was more stable than the wild-type lysozyme, and the extent of the stabilization by each negative charge was found to be additive by measurement of the stability of the wild-type and mutant lysozymes. The additivity may result from the independent contribution of two aspartic acids in the stabilization of the lysozyme such as the formation of hydrogen bonds and the charge-helix microdipole interaction. Moreover, the fixation of WAT1 may be involved in the addition of increased stability in the

18D/27D lysozyme (Fig. III-2 (C)). On the other hand, the extent of stabilization of the lysozyme was not quantitatively consistent with the result of the pK_a of Asp18 or Asp27 in the wild-type and mutant lysozymes. The measurement of stability of lysozymes was carried out in the presence of the concentrated salt. Since the pK_a of Asp18 increased with an increase in ionic strength (*16*), the contribution of the negative charge may be underestimated under the measuring condition of stability. Anyway, it should be the first evidence that two neighboring negative charges at the N-terminus of the helix additively increased the stability of a protein. From the above result, I am sure that these residues in rat, mouse P or mouse M lysozyme contribute to increased stability of the molecule.

REFERENCES

1. Hol, W.G., van, Duijunen, P.T., and Berendsen, H.J. (1978) *Nature*, **273**, 443-445.
2. Richardson, J.S. and Richardson, D.C. (1988) *Science*, **240**, 1648-1652.
3. Shoemaker, K.R., Kim, P.S., York, E.J., and Stewart, J.M. (1987) *Nature*, **326**, 563-567.
4. Sali, D., Bycroft, M., and Fersht, A.R. (1998) *Nature*, **335**, 740-743.
5. Sancho, J., Serrano, L., and Fersht, A.R. (1992) *Biochemistry*, **31**, 2253-2258.
6. Nicholson, H., Becktel, W.J., and Matthews, B.W. (1988) *Nature*, **336**, 651-656.
7. Walter, S., Hubner, B., Hahn, U., and Schmid, F.X. (1995) *J. Mol. Biol.*, **252**, 133-143.
8. Blake, C.C.F., Koenig, D.F., Mair, G.A., North, A.C.T., Phillips, D.C., and Sarma, V.R. (1965) Nature, **206**, 757-761.
9. Brünger, A.T. (1991) *Ann. Rev. Phys. Chem.*, **42**, 197-223.
10. Roussel, A., Fontecilla-Camps, J.C., and Cambillau, C. (1990) *TURBO-FRODO: A new program for protein crystallography and modeling*. Bordeaux, France: XV IUCr Congess.
11. Bundi, A. and Wüthrich, K. (1983) *Biopolymers*, **18**, 285-297.

12. Bodenhauser, H., Koger, H., and Ernst, R.R. (1984) *J. Magn. Reson.*, **58**, 370-388.
13. Kumar, A., Ernst, R.R., and Wüthrich, K. (1980) *Biochem. Biophys. Res. Commun.*, **95**, 1-6.
14. Redfield, C. and Dobson, C.M. (1988) *Biochemistry*, **27**, 122-136.
15. Pace, C.N. (1975) *CNC Crit. Rev. Biochem.*, **3**, 1-43.
16. Abe, Y., Ueda, T., Iwashita, H., Hashimoto, Y., Motoshima, H., Tanaka, Y., and Imoto, T. (1995) *J. Biochem.*, **118**, 946-952.
17. Wishart, D.S., Sykes, B.D., and Richard, F.M. (1992) *Biochemistry*, **31**, 1647-1651.
18. Imoto, T., Forster, L.S., Rupley, J.A., and Tanaka, F. (1972) *Proc. Natl. Acad. Sci. U.S.A.*, **69**, 1151-1155.
19. Zhukovsky, E.A., Mulkerrin, M.G., and Presta, L.G. (1994) Biochemistry, **33**, 9856-9864.
20. Imoto, T., Jonson, L.N, North, A.C.T., Phillips, D.C., and Rupley, J.A. (1972) Vertebrate Lysozymes in *the Enzymes* (Boyer, P.D., ed.) Vol. 7, 3rd ed., pp. 665-868, Academic Press, New York.
21. Canfield R.E., Kammerman, S., Sobel, J.H., and Morgan, F.J. (1971) *Nature NewBiol.*, **232**, 16-17.
22. Cortopassi, G.A. and Wilson, A.C. (1990) *Nucleic Acids Res.*, **18**, 1191-1191.
23. Cross, M., Mangelsdorf, I., Wedel, A., and Renkawitz, R. (1988) *Proc. Natl. Acad. Sci. U.S.A.*, **85**, 6232-6236.
24. White, T.J., Mross, G.A., Osserman, E.F., and Wilson, A.C. (1977) *Biochemistry*, **16**, 1430-1436.

CHAPTER IV

Influence of Mutations of not Conserved N-Cap Residue, Gly4, on Stability and Structure of Hen Lysozyme

ABSTRACT

Hen lysozyme belongs to c-type lysozymes that have three α-helices (A, B, C-helix). Ser24 and Asp88 located at N-cap position in B- and C-helix are almost conserved, but the residue 4 at N-cap position in A-helix is not conserved in the c-type lysozymes. In order to investigate the effect of the mutation at 4th position, I have prepared five mutant lysozymes and examined the stabilities and the structures of mutant lysozymes. In G4P lysozyme, because the structure of side chain at 7th position is apart away from A-helix, G4P was less stable by 2.0 kcal/mol than wild-type. In other mutant lysozymes, although the hydrogen bonds of the amide groups at the N1-N3 positions in A-helix disappeared or the modes of these hydrogen bonds were altered, the stabilities of these mutant lysozymes are almost equal to that of wild-type. Namely, these results may lead us to the conclusion that various mutations at the N-cap position in A-helix can be allowed, because the negative charge of Glu7 at the N-terminus mainly stabilizes A-helix.

INTRODUCTION

The comparative biology is an important method to obtain the information of stability of proteins. For example, the amino acid residue at 62th position is a prolyl residue in the thermophilic RNaseH whereas the corresponding residue is a histidine residue in the mesophilic one (*1*). The amino acid residues at 109th, 121th, 175th, 208th, 261th, 270th, 290th, and 378th positions are prolyl residues in the thermophilic oligo-1,6-glucosidase whereas these corresponding residues are other amino acid residues in the mesophilic one (*2*). These results indicated that the introduction of the prolyl residue made a protein to stabilize. Indeed, in

these two proteins it was reported that the mutations of some amino acid residues to prolyl residues stabilized mesophilic RNaseH and oligo-1,6-glucosidase (*1,2*).

On the other hand, hen lysozyme belongs to c-type lysozymes, and the primary structures in many of the c-type lysozymes have been also determined. The difference in the primary structures of c-type lysozymes correlates with the difference in the activity (*3*) and in stability (CHAPTER III). Moreover, in our laboratory, it has already been constructed a system for the expression and secretion of a matured hen lysozyme from the yeast (*4*). Therefore, hen lysozyme is suitable for the investigation of the effects of the mutations in c-type lysozymes.

Table IV-1. Comparison of primary structure of hen, duck-1, duck-III, chachalaca, human, mouse P, cat milk, pig-I lysozymes around A-helix (5-15) and the N-cap of α-helix.

	1	4[a]	10	20	24[a]	88[a]	References
HEN	KVFGRCELAA	AMKRHGLDNY		S	D		16
DUCK-1 (PEKIN)	--YS------	----L-----		S	D		17
DUCK-III (KAKI)	--YE------	----L-----		S	D		18
CHACHALACA	-IYK------	----Y-----		S	D		19
HUMAN	---E-----R	TL--L-M-G-		S	D		20
MOUSE P	--YN-----R	IL--N-M-G-		K	D		21
CAT MILK[b]	-I-PK----R	KL-AE-MN-F		S	D		
PIG-I	--YD---F-R	IL-KS-M-G-		S	D		22

A-helix

[a]The 4th, 24th, and 88th positions are the N-cap in A-helix (5 - 15), B-helix (25 - 35), and C-helix (89 - 101), respectively. [b]Ito *et al.* unpublished results.

C-type lysozymes have three α-helices (A, B, C-helix). Ser24 at N-cap position in B-helix and Asp88 at N-cap position in C-helix are almost conserved in the c-type

lysozymes, but various amino acids exist at the N-cap position (residue 4) in A-helix (5 - 15) in c-type lysozymes (Table IV-1). Since the residue 4 is apart from the active site cleft, this residue may not contribute to the activity. From the comparison of sequences, Gly, Ser, Glu, Asn, Asp, Pro residues appear at 4th position in c-type lysozymes (Table IV-1, Fig. IV-1). In this chapter, I focus my attraction why the various amino acid can present at 4th position in c-type lysozymes. I prepared five mutant lysozymes such as Gly4Ala (G4A), Gly4Ser (G4S), Gly4Asp (G4D), Gly4Glu (G4E), and Gly4Pro (G4P) lysozyme, and compared their stabilities and structures obtained using X-ray crystallography with those of wild-type lysozyme.

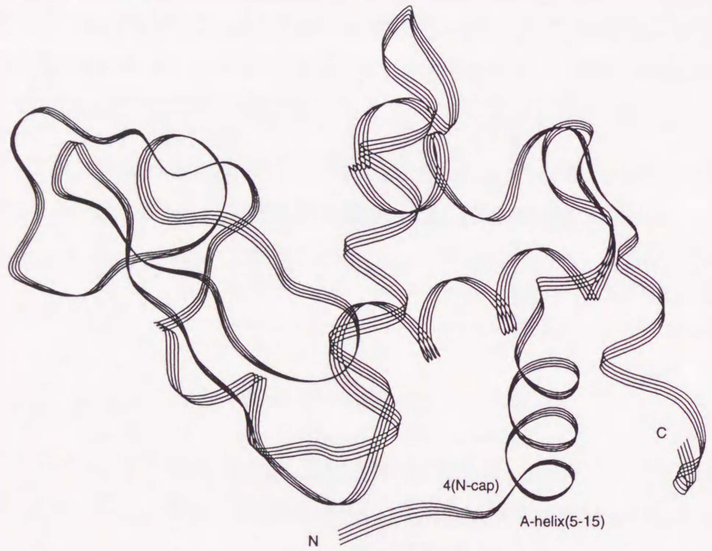

Fig. IV-1. Ribbon drawing of the backbone conformation of hen lysozyme. The residue at 4th position is located at the N-cap in the A-helix (5 - 15) in hen lysozyme.

MATERIALS AND METHODS

Materials.

Restriction enzymes, T4 polynucleotide kinase, DNA polymerase I, DNA sequencing kits, and CM-Toyopearl 650M were the same in CHAPTER I.

Purification and identification of mutant lysozymes secreted by yeast.

Mutant lysozymes (G4A, G4S, G4D, G4E, and G4P lysozyme) were prepared and confirmed by the same procedure in CHAPTER I.

Stabilities of mutant lysozymes determined with Gdn-HCl denaturation.

Unfolding equilibria of mutant lysozymes by guanidine hydrochoride (Gdn-HCl) were measured according to the described procedure in CHAPTER I.

X-ray crystallography of mutant lysozymes.

X-ray crystallograpy of mutant lysozyme was carried out by the same procedure in CHAPTER III.

RESULTS

The stabilities of mutant lysozymes determined with Gdn-HCl denaturation.

The unfolding transition of wild-type lysozyme, G4A, G4S, G4D, G4E, and G4P lysozymes induced by Gdn-HCl were analyzed by observing changes in the tryptophyl fluorescence (emission at 360 nm, excited at 280 nm) as a function of denaturant concentration at pH 5.5 and 35°C. The denaturation of these mutant lysozymes may be explained as an equilibrium between N and D because each lysozyme is one point mutations. Therefore, Gdn-HCl-induced denaturation curves have been analyzed by fitting the data in the equilibrated process (*4*). $\Delta G_D(H_2O)$ is the value of ΔG_D in the absence of Gdn-HCl and m is a measure of the dependence of ΔG_D on Gdn-HCl concentration. The midpoint of Gdn-HCl denaturation is referred to $C_{1/2}$. $\Delta G_D(H_2O)$ was calculated using $C_{1/2}$ and the average m value of wild-type and the mutant lysozymes. The values of $\Delta\Delta G_D$ (H_2O) are calculated by equation (1).

$$\Delta\Delta G_D\,(H_2O) = \Delta G_D(H_2O)_{MUTANT} - \Delta G_D(H_2O)_{WILD} \qquad (1)$$

In Table IV-2, the values of $C_{1/2}$, $\Delta G_D(H_2O)$, and $\Delta\Delta G_D(H_2O)$ of the respective lysozymes as well as m values are summarized. When the stabilities of mutant lysozymes at pH 5.5 were compared with wild-type lysozyme, G4D lysozyme was more stable by 0.2 kcal/mol than wild-type lysozyme, G4S lysozyme had the same stability to wild-type lysozyme, G4A and G4E lysozymes were less stable by 0.3 kcal/mol than wild-type lysozyme, and G4P lysozyme was less stable by 2.0 kcal/mol than wild-type lysozyme. The stabilities of mutant lysozymes except for G4P lysozyme were similar to that of wild-type lysozyme. On the other hand, in comparison of stability between G4D and G4E lysozyme where Gly is mutated to the negatively charged residues, G4D lysozyme was more stable by 0.5 kcal/mol than G4E lysozyme.

Table IV-2. Thermodynamic parameters characterizing the Gdn-HCl denaturation of mutant lysozymes at pH 5.5 and 35°C.

Lysozyme	$C_{1/2}$ (M)	m (kcal/mol/M)	ΔG_D (H_2O)[a] (kcal/mol)	$\Delta\Delta G_D$ (H_2O)[b] (kcal/mol)
G4G (Wild)	3.62±0.01	2.7	10.1	0
G4A	3.53±0.01	2.7	9.8	-0.3
G4S	3.62±0.01	2.9	10.1	0
G4D	3.67±0.02	2.8	10.3	0.2
G4E	3.53±0.01	2.7	9.8	-0.3
G4P	2.88±0.03	3.1	8.1	-2.0

[a]The value is evaluated by using the mean value of m (2.8). [b]$\Delta\Delta G_D$ (H_2O) based on wild-type lysozyme.

Crystal structures of mutant lysozymes.

The crystallographic data collection and refinement statistics for the crystal structures of wild-type and mutant lysozymes are summarized in Table IV-3. The refined structures of these mutant lysozymes were in good agreement with that of wild-type lysozyme. Superimposing each mutant lysozyme on wild-type lysozyme, I calculated the root mean square (r.m.s.) deviation in coordinates of main chains to be 0.07Å for G4A, 0.10Å for G4S, 0.11Å for G4D, 0.11Å for G4E, and 0.11Å for G4P lysozyme, respectively.

Table IV-3. Crystallographic data collection and refinement statistics of lysozymes.

Lysozyme	G4G[a] (Wild)	G4A[a]	G4S[a]	G4D[b]	G4E[b]	G4P[a]
Data collections						
Cell dimensions						
a,b (Å)	79.21	79.10	79.05	78.84	78.72	79.24
c (Å)	37.97	38.12	38.06	38.21	38.43	37.83
Resolution (Å)	1.75	1.87	1.86	1.82	1.82	1.86
Unique reflections [F>1σ(F)]	11948	9877	8948	10035	10120	9486
Completeness (%)	93.2	93.2	83.7	88.8	89.0	89.2
R-merge (%)[c]	3.69	4.76	8.30	7.97	5.23	5.93
Refinement						
R-factor (%)[d]	16.8	17.1	17.4	17.3	17.4	17.3
Δ bond length (Å)	0.009	0.009	0.010	0.010	0.009	0.010
Δ bond angle (°)	1.448	1.475	1.513	1.500	1.486	1.534
Number of water molecules	98	68	71	64	64	62

[a]These lysozymes are crystallized at pH 4.7. [b]These lysozymes are crystallized at pH 6.5. [c]R-merge=$\Sigma|Fi-F|/\Sigma Fi$, where Fi are repeated measurements of equivalent structure amplitudes and F is the average value of Fi. [d]R-factor=$\Sigma|Fobs-Fcalc|/\Sigma Fobs$.

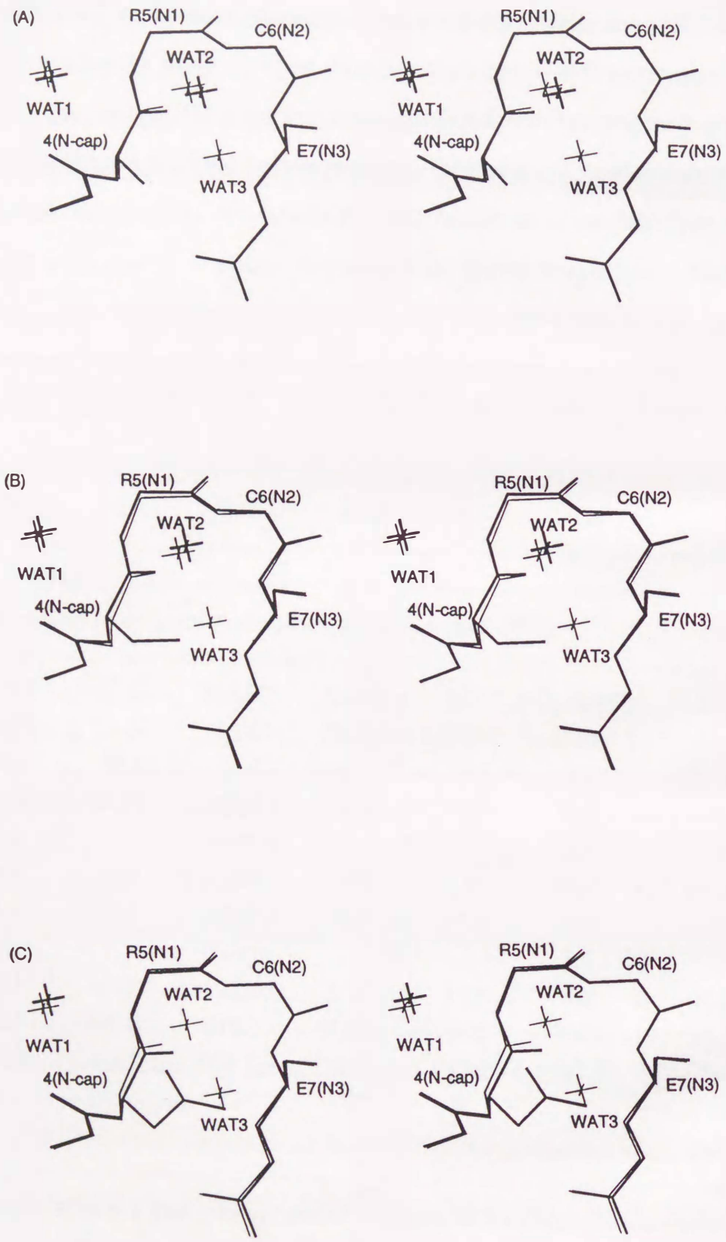

Fig. IV-2. Superposition of the structures of each lysozyme (thick line) on that of wild-type lysozyme (thin line). The amide group at the N1, N2, and N3 position form hydrogen bond with WAT1, WAT2, and WAT3, respectively. (A) is G4A lysozyme, (B) is G4S lysozyme, (C) is G4D lysozyme, (D) is G4E lysozyme, and (E) is G4P lysozyme.

(1) G4G lysozyme (Wild-type): The N-terminal neighbor of A-helix in wild-type lysozyme (thin line) is shown in Fig. IV-2 (A). The amide groups at the N1, N2, and N3 positions in A-helix in wild-type lysozyme formed hydrogen bonds with three water molecules (WAT1, WAT2, and WAT3), respectively (Table IV-4).

(2) G4A lysozyme: The N-terminal neighbor of A-helix in G4A lysozyme (thick line) is shown in Fig. IV-2 (A). The amide groups at the N1 and N2 positions in A-helix in G4A lysozyme formed hydrogen bond with two water molecules (WAT1 and WAT2), respectively. The amide groups at the N3 position did not form a hydrogen bond (Table IV-4).

(3) G4S lysozyme: The N-terminal neighbor of A-helix in G4S lysozyme (thick line) is shown in Fig. IV-2 (B). The amide groups at the N1, N2, and N3 positions in A-helix in G4S lysozyme formed hydrogen bond with two water molecules (WAT1 and WAT2) and the side chain of Ser4, respectively (Table IV-4). Therefore, the two hydrogen bonds between backbones and side chains at the N-cap and N3 positions (Ser4 and Glu7) was found to form the Capping Box (5).

Table IV-4. Hydrogen bonding of the amide groups at the N1, N2 and N3 positions in A-helix of lysozymes.

		Distance (Å)					
H - donor	H - acceptor	G4G (Wild)	G4A	G4S	G4D	G4E	G4P
Arg5 N (N1)	WAT1	3.00	2.78	2.85	2.88	2.81	2.95
	Asp4 Oγ1				2.82		
Cys6 N (N2)	WAT1	2.93	2.85	2.85			2.87
	Glu4 Oε1					2.91	
Glu7 N (N3)	WAT3	3.15					
	Ser4 Oγ			3.27			
	Asp4 Oγ2				3.21		
	Glu4 Oε2					3.00	

(4) G4D lysozyme: The N-terminal neighbor of A-helix in G4D lysozyme (thick line) is shown in Fig. IV-2 (C). The amide group at the N1 position in A-helix in G4D lysozyme formed hydrogen bond with one water molecule (WAT1) or the side chain of Asp4. The amide groups at the N2 position did not form a hydrogen bond (Table IV-4). The amide group at the N3 position in A-helix in G4D lysozyme formed hydrogen bond with the side chain of Asp4. The view from N-terminus of A-helix in G4D (thick line) and G4E lysozyme (thin line) is

shown in Fig. IV-3. The side chain of Asp4 in G4D lysozyme was located closer to the center of A-helix than that of Glu4 in G4E lysozyme.

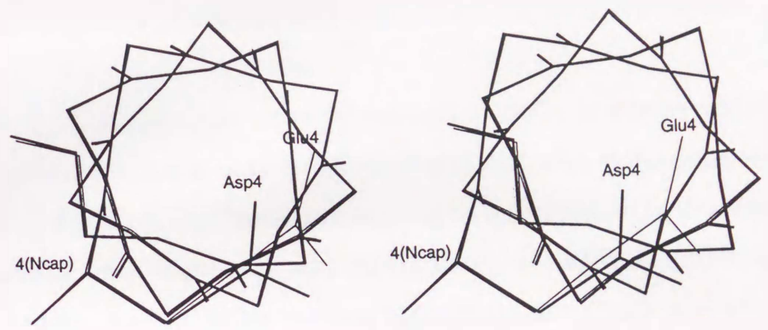

Fig. IV-3. Showing of the crystal structure of the region near N-terminus of A-helix (5-15) in G4D (thick line) and G4E lysozyme (thin line).

(5) G4E lysozyme: The N-terminal neighbor of A-helix in G4E lysozyme (thick line) is shown in Fig. IV-2 (D). The amide group at the N1 position in A-helix in G4E lysozyme formed hydrogen bond with one water molecule (WAT1). The amide group at the N2 and N3 positions in A-helix in G4E lysozyme formed hydrogen bond with the side chain of Glu7 (Table IV-4).

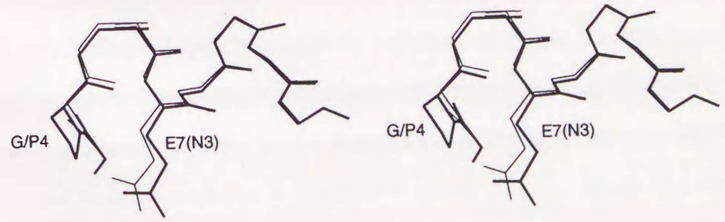

Fig. IV-4. Showing of the crystal structure of the region near N-terminus of A-helix (5-15) in G4P (thick line) and wild-type lysozyme (thin line).

(6) G4P lysozyme: The N-terminal neighbor of A-helix in G4P lysozyme (thick line) is shown in Fig. IV-2 (E). The amide groups at the N1 and N2 positions in A-helix in G4P lysozyme formed hydrogen bond with two water molecules (WAT1 and WAT2), respectively. The amide groups at the N3 position did not form a hydrogen bond (Table IV-4). Because of the mutation of Pro4, the orientation of the side chain of Glu7 was apart away from A-helix (Fig. IV-4).

DISCUSSION

Using crystallographic data, Richardson, J.S. and Richardson, D.C. have reported that the amino acid residues such as Asn, Ser, Asp and Gly frequently exist at the N-cap position in α-helix (*6*). Some scientists have investigated the stabilities of mutant proteins where the amino acid residue at the N-cap position was mutated to the above amino acid. From the result of their studies on barnase (*7*), T4 lysozyme (*8*), growth hormone (*9*), and histidine-containing protein (*10*), these mutant proteins where the amino acid residue at the N-cap positions was mutated to Asp or Glu were more stable than the mutant protein where the amino acid residue in question was mutated to Ala due to the charge helix microdipole interaction. On the other hand, from the result of their studies on barnase (*7*), T4 lysozyme (*8*), and histidine-containing protein (*10*), these mutant proteins where the amino acid residue at the N-cap positions was mutated to Ser or Thr were more stable than the mutant protein where the amino acid residue in question was mutated to Ala due to the end capping effect. In this chapter, I investigated the structures and stabilities of mutant lysozymes where the amino acid residue at 4th position was mutated to Ala, Ser, Asp, Glu, and Pro, because there were various amino acids in nature at this position in c-type lysozymes. The stabilities of mutant lysozymes except for G4P lysozyme were similar to that of wild-type lysozyme.

So far, the experimental results (*8-11*) reported that the electrostatic interaction between the charged side chain at the N-cap position and helix microdipole stabilized proteins. This was consistent with the present result that G4D

lysozyme was slightly more stable than wild-type lysozyme, and G4E lysozyme was less stable than wild-type lysozyme. Since the side chain of Asp4 in G4D lysozyme was located closer to the center of the A-helix than that of Glu4 in G4E lysozyme (Fig. IV-3), the helix-charge microdipole interaction in G4D lysozyme was stronger than that in G4E lysozyme. The difference in the structures between G4D and G4E lysozymes may be involved in the difference in the stabilities between those lysozymes.

However, from the reports on barnase (*7*) and T4 lysozyme (*11*), it was demonstrated that the mutant proteins where the residue at the N-cap position was mutated to Asp and Glu were more stable by a range 0.4 to 1.5 kcal/mol than the mutant protein where this residue was mutated to Gly. If the charge-helix microdipole interaction between the charged side chain at 4th position and A-helix had contributed to the stabilization in G4D and G4E lysozyme, these mutant lysozymes should be more stable. Therefore, there may be a destabilizing factor around the N-terminus of A-helix. From the reports on hen lysozyme, the mutant lysozyme where Glu7 was mutated to Gln was less stable by 1.2 kcal/mol than wild-type lysozyme (*12*), and the mutant lysozyme where Asn27 was mutated to Asp was more stable by 0.4 kcal/mol than wild-type lysozyme (CHAPTER III). Since 7th and 27th positions were located at N3 position in A-helix and B-helix, respectively, in hen lysozyme, the charge-helix microdipole interactions between the charged side chain at the N3 position and α-helix should contribute to the stabilization in hen lysozyme. The negative charge at Glu7 mainly stabilizes A-helix at the N-terminus of lysozyme. Moreover, as the distance between the side chains at the N-cap and N3 positions was very short, it may be considered that the electrostatic repulsion between these side chains occur, resulting that the extent of the practical stabilization was smaller than that of the expected stabilization in G4D and G4E lysozymes.

The structures of G4A and G4S lysozymes were different from that of wild-type lysozyme while the stabilities of them were almost similar. In G4A lysozyme, the hydrogen bond between the amide group at the N3 position (residue 7) in A-

helix and WAT3 water molecule was found to disappear. In G4S lysozyme, the WAT3 water molecule was replaced by the hydroxyl group of Ser4. The hydroxyl group of Ser4 in G4S lysozyme formed the end capping which was the hydrogen bond between the amide group at the N3 position and the side chain at the N-cap position. Therefore, the reason why the stabilities of G4A and G4S lysozymes were similar to that of wild-type lysozyme may depend that the N-terminal neighborhood (N1, N2, and N3) in A-helix of hen lysozyme was exposed to solvent molecules. Thus, the stabilities of G4A, G4S, G4D, and G4E lysozymes were similar to that of wild-type lysozyme, and several mutations of the amino acid residue at 4th position in c-type lysozymes were attainable without affecting the stability of global structure.

On the other hand, Nicholson *et al.* have suggested that when a protein was stabilized by replacing some amino acid residue with prolyl one, the dihedral angles of the residue proceeding the introducing proline and the introduced prolyl residue should be considered (*13*). The dihedral angles of the amino acids at 3rd and 4th positions in wild-type lysozyme are in allowed ranges. However, G4P lysozyme was less stable by 2.0 kcal/mol than wild-type lysozyme. In the structure of G4P lysozyme, the hydrogen bond between the amide group at 4th position and the side chain at 7th position was found to disappear. Consequently, one reason for the instability in G4P lysozyme may depend on the loss of the hydrogen bond. However, as Shirley *et al.* demonstrated that most of intramolecular hydrogen bonds contributed 1.3 ± 0.6 kcal/mol to the stability of structures such as globular proteins (*14*), the extent of the instability in G4P lysozyme was larger than that of stability of one hydrogen bond. The mutant lysozyme where Glu7 was mutated to Gln was less stable by 1.2 kcal/mol than wild-type lysozyme due to loss of this charge-helix microdipole interaction (*12*). From X-ray crystallography, the orientation of the side chain of Glu7 was apart away from N-terminus of A-helix in G4P lysozyme. Consequently, the other reason for the instability in G4P lysozyme may depend on decrease in the charge-helix microdipole interaction between the charged side chain at 7th position and

A-helix. In cat milk lysozyme, amino acid residue at 4th position is a Pro. This cat milk lysozyme has a calcium binding site (86-92). Because lysozymes which have calcium binding sites were stable (*15*), it is consider that Pro residue at the N-cap position in A-helix can be allowed.

Finally, I refer to the reason why various amino acids are present at 4th position in c-type lysozymes. From the result above, several mutations of amino acid at 4th position did not affect the stabilization of A-helix in c-type lysozymes. As was shown above, the negative charge at Glu7 stabilized lysozyme (*12*). The extent was estimated to be 1.2 kcal/mol. This value was larger than the fluctuation of the stability of mutant lysozyme where Gly4 was mutated to Ala, Ser, Asp, and Glu, respectively. These results may lead us to the conclusion that various mutations at the N-cap position in A-helix can be allowed, because the negative charge of Glu7 at the N-terminus mainly stabilizes A-helix .

REFERENCES

1. Ishikawa, K., Kimura, S., Kanaya, S., Morikawa, K., and Nakamura, H. (1993) *Protein Eng.*, **6**, 85-91.
2. Watanabe, K., Masuda, T., Ohashi, H., Mihara, H., and Suzuki, Y. (1994) *Eur. J. Biochem.*, **226**, 277-283
3. Kumagai, I., Sunada, F., Takeda, S, and Miura, K. (1992) *J. Biol. Chem.*, **267**, 4608-4612.
4. Pace, C.N. (1975) *CNC Crit. Rev. Biochem.*, **3**, 1-43.
5. Haper, E.T., and Rose, G.D. (1993) *Biochmistry*, **32**, 7605-7609.
6. Richardson, J.S. and Richardson, D.C. (1988) *Science*, **240**, 1648-1652.
7. Serrano, L. and Fersht, A.R. (1989) *Nature*, **342**, 296-299.
8. Bell, J,A., Becktel, W.J., Sauer, U., Baase, W.A., and Matthews, B.W. (1992) *Biochemistry*, **31**, 3590-3596.
9. Zhukovsky, E.A., Mulkerrin, M.G., and Presta, L.G. (1994) *Biochmistry*, **33**, 9856-9864.

10. Thapar, R., Nicholson, E. M., Ponni Rajagopal, P., Waygood, E. B., Scholtz, J. M., and Klevit, R. E. (1996) *Biochemistry*, **35**, 11268-11277.

11. Nicholson, H., Becktel, W. J., and Matthews, B. W. (1988) *Nature*, **336**, 651-656.

12. Abe, Y., Ueda, T., Iwashita, H., Hashimoto, Y., Motoshima, H., Tanaka, Y., and Imoto T. (1995) *J. Biochem.*, **118**, 946-952.

13. Nicholson, H., Tronrud, D. E., Becktel, W. J., and Matthews B. W. (1992) *Biopolymers*, **32**, 1431-1441.

14. Shirley, B.A., Stanssens, P., Hahn, U., and Pace, C.N. (1992) *Biochemistry*, **31**, 725-732.

15. Kuroki, R., Taniyama, Y., Seko, C., Nakamura, H., Kikuchi, M., and Ikehara, M. (1989) *Proc. Natl. Acad. Sci. U.S.A.*, **86**, 6903-6907.

16. Imoto, T., Jonson, L.N, North, A.C.T., Phillips, D.C., and Rupley, J.A. (1972) Vertebrate Lysozymes in *the Enzymes* (Boyer, P.D., ed.) Vol. 7, 3rd ed., pp. 665-868, Academic Press, New York.

17. Kondo, K., Fujio, H., and Amno, T. (1982) *J. Biochem.*, **91**, 581-587.

18. Hermann, J., Jolles, J., and Jolles, P. (1971) *Eur. J. Biochem.*, **24**, 12-17.

19. Jolles, J., Parger, E.M., Shoentgen, F., and Wilson, A.C. (1976) *J. Mol. Evol.*, **8**, 59-78.

20. Canfield R.E., Kammerman, S., Sobel, J.H., and Morgan, F.J. (1971) *Nature New Biol.*, **232**, 16-17.

21. Cortopassi, G.A. and Wilson, A.C. (1990) *Nucleic Acids Res.*, **18**, 1191-1191.

22. Jolles, J., Jolles, P., Bowman, B.H., Prager, E.M., Stewart, C.B., and Wilson, A.C. (1989) *J. Mol. Evol.*, **28**, 528-535.

CONCLUSION

In this thesis, I showed that amino acid mutations and X-ray crystallography are useful methods to analyze the relationship between the stability and the structure in proteins.

In CHAPTER I, although Gly-Pro mutant lysozyme was not always more stable than Pro-Gly mutant lysozyme, it was found that the differences in the free energy changes between Gly-Pro and Pro-Gly mutant lysozyme at same site caused by the differences in their energy-levels in the folded states.

In CHAPTER II, I showed ϕ-values using the differences in free energy change and in activation free energy change between Gly-Pro and Pro-Gly mutant lysozyme. These ϕ-values gave information on how much the mutated sites retained the folded structure in the transition state of unfolding. Based on the values, it was found that a considerable portion of the structure at residues 121-122 in the 3_{10}-helix was retained in the transition state and the β-sheet structure was moderately disrupted while both the β-turn and the loop were considerably unfolded. The information on the structure in the transition state in the unfolding of hen lysozyme was novel. Moreover, this method should be applicable for analyzing the transition states of other proteins.

In CHAPTER III, the stabilities, the structures, and the pK_as of introduced Asp residue in mutant lysozyme where 18th and/or 27th positions are mutated to Asx were analyzed. From these results, two neighboring negative charges at N-terminus of the helix additionally was shown to contribute to increased stability of a protein using X-ray crystallography and NMR.

In CHAPTER IV, the stabilities and the structures in mutant lysozyme where 4th positions is mutated to various amino acids were examined. Since some mutant lysozymes at 4th position had similar stability, it was suggested that

various mutation at the N-cap position (residue 4) in A-helix could be allowed because the negative charge of Glu7 at the N-terminus mainly stabilizes A-helix.

In conclusion, I described the structure in the transition state of hen lysozyme by developing the novel method and discussed the stabilities of mutant lysozymes based on their structure. I believe that the information obtained here may be helpful in constructing stable proteins which are long-lived in vivo and retain their activity for a long time.

ACKNOWLEDGMENTS

I would like to thank Prof. T. Imoto of Graduate school of Pharmaceutical Science, Kyushu University, for helpful suggestion, guidances, and advices throughout the course of this work and critical reading of this thesis. I wish to thank Associated Prof. T. Ueda of Graduate school of Pharmaceutical Science, Kyushu University, for his earnest guidances throughout the experimental work and for his useful discussions. I wish to thank Dr. Y. Ito, Mr. Y. Hashimoto, Dr. H. Tomizawa, Dr. Y. Abe, and Dr. Y. Maeda for their useful suggestions. I wish to thank Dr. T. Yamane, Dr. Y. Hata, Dr. R. Kuroki, and T. Shimizu for their helpful suggestions X-ray crystallography. I wish to thank Mr. Iwashita, Mr. Oumura, Mr. Mine, Miss Tsutsumi, Miss Mukae, Miss Chijiiwa, and Mr. Masumoto for their experimental assistances. I wish to thank co-workers in my laboratory for their friendship and sincere supports in various directions.